



Multiple Quaternary erosion and infill cycles in overdeepened basins of the northern Alpine foreland

Marius W. Buechi¹ · Hans Rudolf Graf² · Peter Haldimann³ · Sally E. Lowick¹ · Flavio S. Anselmetti¹

Received: 29 August 2016 / Accepted: 24 November 2017 / Published online: 18 December 2017
© Swiss Geological Society 2017, corrected publication 01/2018

Abstract

The cumulative effect of repeated extensive glaciations represents a poorly constrained component in the understanding of landscape evolution in mid-latitude mountain ranges such as the Alps. Timing, extent, and paleo-climatic conditions of these glaciations are generally poorly understood due to the often-fragmentary character of terrestrial Quaternary records. In this context, the sedimentary infills of subglacial basins may serve as important archives to complement the Quaternary stratigraphy over several glacial–interglacial cycles. In this study, sedimentary facies, valley-fill architecture, and luminescence dating are used to describe nine erosional and depositional cycles (Formations A–I) in the Lower Glatt valley, northern Switzerland. These cycles can be related to the ‘Birrfield’ Glaciation (~ MIS2), the ‘Beringen’ Glaciation (~ MIS6), and up to three earlier Middle Pleistocene glaciations that can be tentatively correlated to the regional glaciation history. Evidence suggests that deep bedrock trough incision and/or partial re-excavation last occurred mainly during the ‘Beringen’ and ‘Habsburg’ Glaciations. Second-order, ‘inlaid’ glacial basins document separate glacier readvances during the Beringen Glaciation. The arrangement of subglacial basins in the Glatt valley with different sub-parallel or bifurcating bedrock troughs, re-excavated segments, and inlaid basins document changes in the magnitude and the spatial focus of subglacial erosion over time. The Glatt valley may thus serve as a key example for the glacial landscape evolution in many other repeatedly glaciated forelands.

Keywords Landscape evolution · Overdeepening · Glaciation history · Northern Alpine foreland · Glacial basin stratigraphy · Luminescence dating

1 Introduction

Mid-latitude mountain ranges such as the Alps have been shaped by repeated Pleistocene glaciations (e.g. Penck 1905). While the effects of the most recent glaciation tend to dominate the geomorphological processes in Alpine

landscapes at present (Schlunegger and Norton 2013; Salcher et al. 2014), the glacial landscapes are most likely the cumulative product of repeated glaciation during the Pleistocene. It is thus essential to better constrain number, extent, and timing of all glaciations during this period to understand how Alpine landscapes have evolved under this influence. The reconstruction of such complete glaciation histories is challenging as terrestrial Quaternary archives are often characterized by only discontinuous deposition and fragmentary preservation (e.g. Rose and Menzies 2002). However, longer sedimentary sequences may be preserved over several glacial cycles in deep glacial basins. At valley-scale, these glacial basins are in the order of tens or hundreds of meters deep, and can be several kilometres long (e.g. Schlüchter 1979; van Husen 1979). These basins are typically subglacially ‘overdeepened’, i.e. eroded below the regional base level, which causes a relatively large accommodation space upon deglaciation, and an overall increase of the preservation potential (Preusser

Editorial handling: Christian Schlüchter.

Electronic supplementary material The online version of this article (<https://doi.org/10.1007/s00015-017-0289-9>) contains supplementary material, which is available to authorized users.

✉ Marius W. Buechi
marius.buechi@geo.unibe.ch

¹ Institute of Geological Sciences and Oeschger Centre for Climate Change Research, University of Bern, Bern, Switzerland

² Dr. von Moos AG, Zurich, Switzerland

³ Dr. Heinrich Jäckli AG, Zurich, Switzerland

et al. 2010; Cook and Swift 2012). While glaciations after the first erosion-infilling cycle may re-excavate these valley fills, partial preservation over several glacial cycles is not uncommon (see Preusser et al. 2010). In the case of partial preservation, the resulting sequences of glacial and (glacio)-lacustrine deposits may thus provide more complete sedimentary archives for the glaciation and environmental history. The scientific value of overdeepened glacial basins as Quaternary archives has been demonstrated at relatively few sites, where sequences spanning over one to several glaciations were recovered from strategically placed drill sites (e.g. Schlüchter 1989; Preusser et al. 2005; Anselmetti et al. 2010; Dehnert et al. 2012; Stamberger et al. 2013; Fiebig et al. 2014). In combination with modern dating techniques (mostly luminescence dating and/or pollen stratigraphy), these studies have significantly improved the understanding of the Middle and Late Pleistocene glaciations and interglacial/interstadial periods in the 'proximal' glaciated areas of the Alps. Moreover, these results are significant for applied hydrogeology and engineering geology purposes, as underground exploration and construction increasingly involve deposits hosted in overdeepened basins as well.

The Lower Glatt valley (LGV), located on the northern Swiss Plateau (Fig. 1), has long been considered one of the key regions for the Middle to Late Pleistocene glaciation history of the northern Alpine foreland and has been documented over several generations of research (e.g. Hug 1907; Penck and Brückner 1909; Weber 1928, 1934; Beck 1933; Hug and Beilick 1934; Suter 1944; Hantke 1959; Freimoser and Locher 1980; Graf 2009; Preusser et al. 2011). While the overdeepened character and the likely pre-last glacial age of many LGV sediments have been acknowledged since the 1970s (Wyssling and Wyssling 1978; Haldimann 1978; Freimoser and Locher 1980), five fully cored drill holes commissioned by the environmental authorities of the Canton of Zurich (AWEL) in 2011/2012, gave unprecedented access to these deeply buried basin structures. Based on these cores, we reconstruct the landscape and subglacial basin evolution of the Lower Glatt valley by identifying erosional and depositional cycles through detailed sedimentary facies analysis in drill cores and outcrops, luminescence dating, and integration of important tie-points up- and down-valley of the study site.

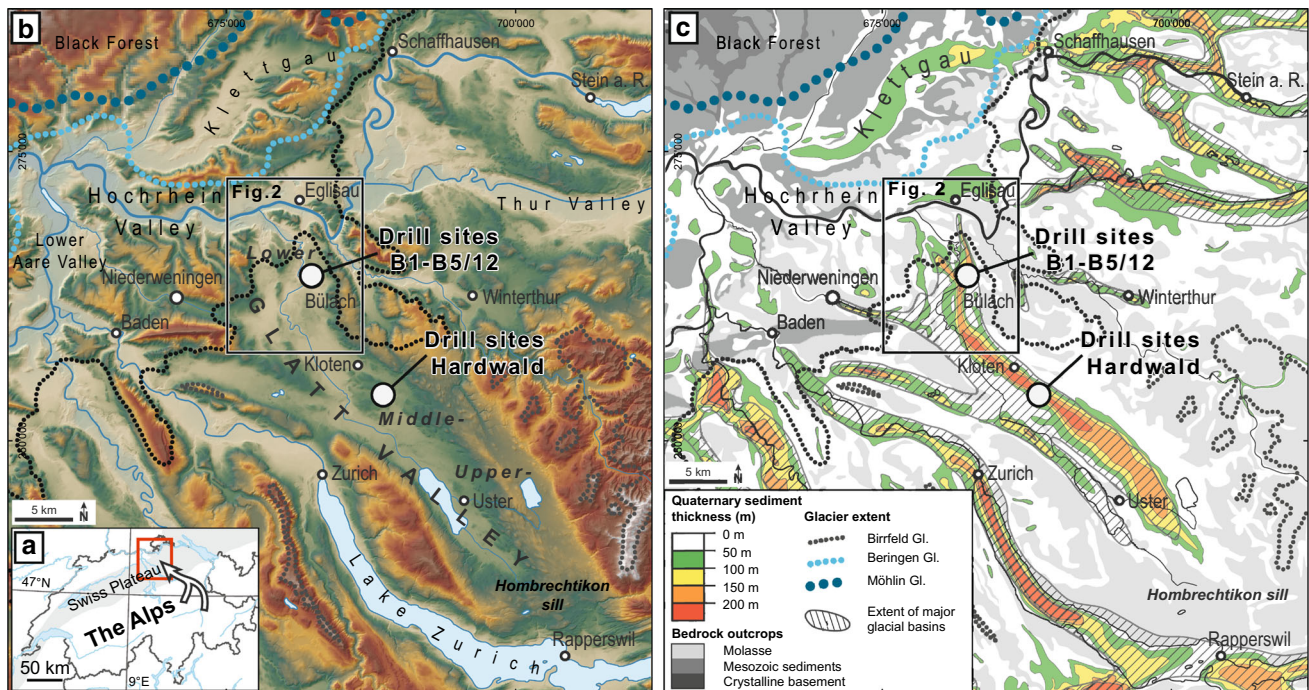


Fig. 1 **a** Location of the Glatt valley in the northern Swiss Plateau; the arrows mark the dominant ice flow directions for the Glatt valley glacier originating in the Glarus and Graubünden Alps. **b** Location of the main drill sites (and other sites referred to in the text, elevation data: DHM25 © Swisstopo). **c** Map of the same extent as **(b)** reveals thick Quaternary sediment accumulation in buried glacially

overdeepened basins (bedrock surface model compiled by Pietsch and Jordan 2014; modern lakes are filled). The thickest sediments occur within the extent of the major glacial basins (modified after Graf 2009). The maximum extent of the Möhlin, Beringen, and Birrfeld Glaciations are shown. After Bini et al. (2009), Graf (2009, and Preusser et al. (2011)

2 Geologic background

2.1 Overall setting and glaciation history

The Glatt valley (Fig. 1a) is a 6–8 km wide valley with a glacially-shaped landscape typical for the northern Swiss plateau (e.g. Bodenburg Hellmund 1909; Stein 1948; Jung 1969). The Glatt valley extends in a north-westerly direction from a broad bedrock sill at ~ 510 m a.s.l., separating it from the upper Lake Zurich basin (Hombrechtikon sill), to the Hochrhein valley at its northern end (Fig. 1b). During extensive Pleistocene glaciation of northern Switzerland, glaciers originating from the Glarus and Graubünden Alps repeatedly advanced into the Swiss Plateau and overflowed the Hombrechtikon sill to form a Glatt valley glacier lobe (see e.g. Keller and Krayss 2005; Preusser et al. 2011). Maximum glacier extents during the last glacial cycle (Birrfeld Glaciation, Preusser et al. 2011) reached as far as the LGV (Fig. 1) and much of the present glacial geomorphology can be attributed to this glaciation and its retreat stages (e.g. Keller and Krayss 2005). The Middle Pleistocene glacier extents are poorly constrained but evidence suggests that during the penultimate glaciation (Beringen Glaciation, MIS6, Preusser et al. 2011), the Glatt valley glacier, together with adjacent lobes, may have advanced several kilometres into the Hochrhein valley (Fig. 1). Before the Beringen Glaciation the area was likely glaciated at least twice during the Middle Pleistocene by the Habsburg glaciation, which was probably of similar extent as the Birrfeld glaciation, and the most extensive Möhlin Glaciation (Fig. 1; Preusser et al. 2011).

2.2 Overview of the Quaternary depositional record

The surface geology and geomorphology in the LGV (Fig. 2a) are dominated by deposits of the Birrfeld Glaciation. These deposits comprise a broad terminal moraine complex and extensive outwash gravel plains extending northwards into the Hochrhein valley (e.g. Keller and Krayss 2005). The terminal moraine complex is most likely the result of a multi-phase glacier retreat and stabilization as indicated by a succession of terminal and lateral moraines (e.g. Weber 1928; Sommerhalder 1968) including local glacier-overriding and interfingering with the outwash plain (e.g. Hantke 1967; Freimoser and Locher 1980). Tills deposited during an early far-reaching advance are buried beneath younger outwash deposits (defining the LGM as shown in Bini et al. 2009; Graf 2009), while a morphologically prominent terminal moraine is preserved between the villages of Stadel and Bülach. Additional moraine morphologies are nested within the

tongue basin and mark later retreat stages (e.g. Neerach–Hochfelden and Hofstetten–Oberglatt–Seeb, see Fig. 2b).

Glacigenic deposits outside the limits of the last glaciation (Fig. 2; e.g. on the hills east of Bülach) and elevated outwash plain relicts can be broadly attributed to Middle Pleistocene glaciation periods. The plateau between Strassberg and Chatzenstig northwest of Bülach (hereafter termed ‘Strassberg Plateau’) is the most prominent Middle Pleistocene outwash plain relict, with an extent of at least ~ 3 km² and potential terrace equivalents between Zweidlen and Glattfelden (e.g. du Pasquier 1891; Weber 1928, 1934; Suter 1944; Graf 2009). The oldest Quaternary deposits consist of Early Pleistocene fluvial and fluvio-glacial sediments of the Higher and Lower Deckenschotter Group that cover the flat-topped Molasse hills surrounding the Lower Glatt valley (e.g. Graf 1993).

2.3 Bedrock topography and geology

Bedrock outcrops are limited to gentle hills enclosing the LGV and a few isolated bedrock highs that rise above the valley floor. For the rest, the bedrock surface topography is strongly depressed below the valley bottom similar to the neighbouring valleys (Fig. 1b). Systematic drilling campaigns for groundwater purposes (e.g. Freimoser and Locher 1980; Kempf et al. 1986) revealed elongated bedrock depressions buried below up to ~ 200 m of Quaternary sediments (Fig. 1c). These bedrock troughs are eroded well below the regional fluvial base level and terminate abruptly with reverse slopes. In the absence of tectonic features explaining these bedrock lows they are interpreted as overdeepened subglacial basins (Freimoser and Locher 1980; Graf 2009; Buechi et al. 2017a). The Upper and Middle Glatt valley are largely dominated by one relatively broad bedrock trough (see also Green et al. 2013), while several narrow bedrock troughs can be discerned inset within the broad valley cross-section in the Lower Glatt valley (Fig. 2b).

The geometric relationship of these different bedrock troughs in the LGV is not well understood. While it may be assumed that they are more or less continuous features (e.g. Jordan 2010; Dürst Stucki and Schlunegger 2013), the connections between the individual overdeepened trough elements are often poorly constrained, and will be discussed later. In the LGV, the following individual features can be identified (see Fig. 2b):

- Bülach Trough: a S–N trending bedrock trough between Bülach and Eglisau.
- Strassberg Trough: a shorter NW-trending feature, closing to the northwest.

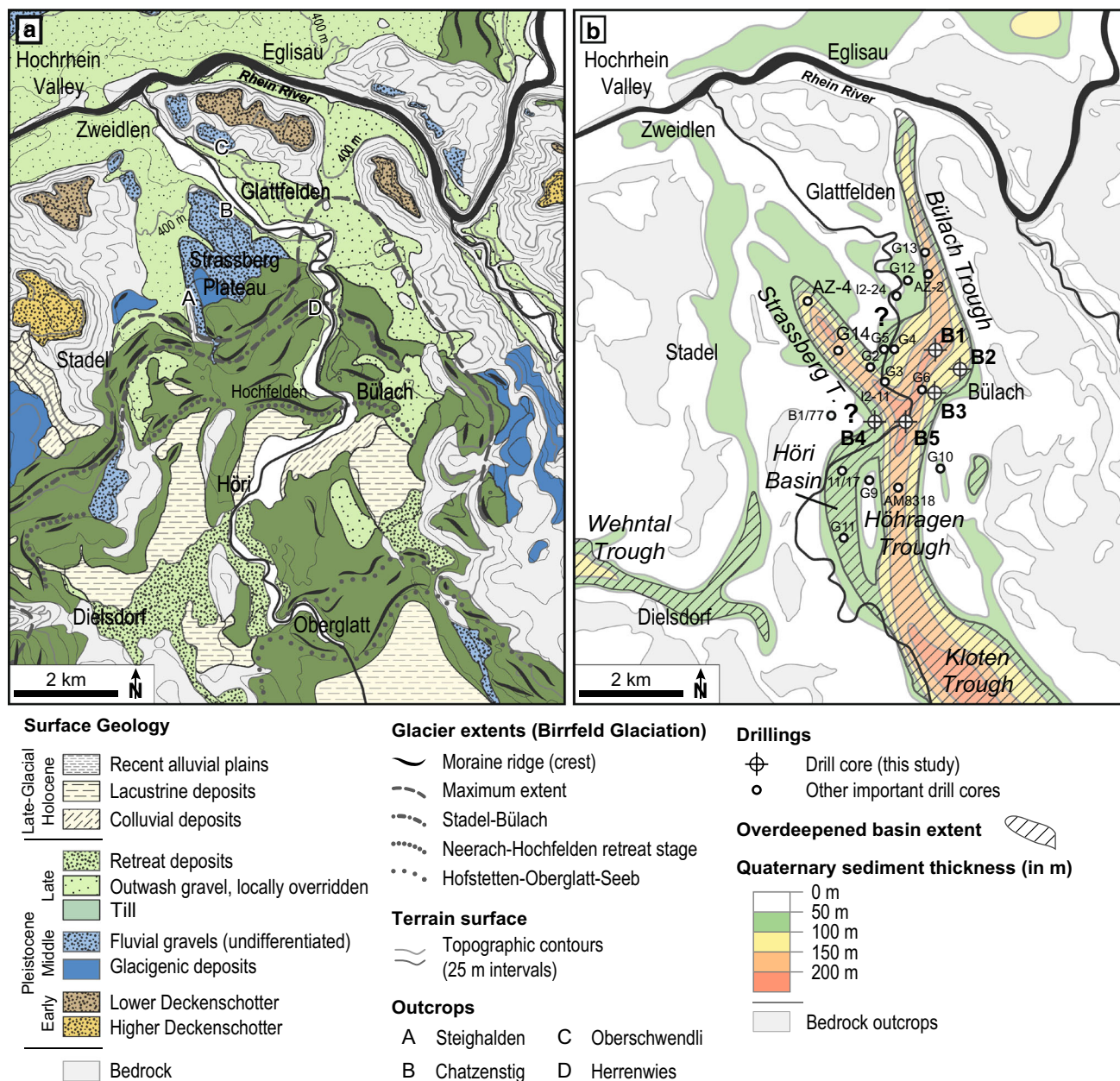


Fig. 2 **a** Geological map of the Lower Glatt valley with locations referred to in the text. **b** Quaternary sediments (up to 200 m thick) are infilled into several distinct overdeepened bedrock troughs. Geology

after Isler et al. (1984), Sommerhalder (1968), Hantke (1967), and own observations. Bedrock surface model compiled by Pietsch and Jordan (2014)

- Höhragen Trough: a deep, but poorly constrained bedrock trough, which could be considered as a link between the Bülach Trough and the Klotten Trough.
- Klotten Trough: a deep bedrock trough south of Oberglatt, which extends further SE into the Middle Glatt valley (see Haldimann 1978; Kempf et al. 1986).
- Höri Basin: a broadly parallel, but less overdeepened feature, therefore named ‘basin’, to the west.
- Wehntal Trough: the easternmost section of a bedrock trough in the Wehntal between Dielsdorf and

Niederweningen (see Anselmetti et al. 2010; Dehnert et al. 2012).

All the trough elements in the LGV (Fig. 2b) are incised into bedrock dominated by sandstones and mudstones of the Swiss Molasse basin. These Miocene fluvio-terrestrial and shallow marine sedimentary rocks are often poorly consolidated and of low erosional resistance (Kühni and Pfiffner 2001). In the Upper Glatt valley and towards the Hombrechtikon bedrock sill, less erodible conglomerate beds gradually dominate (e.g. Zingg 1934; Wyssling 2008).

3 Methods

3.1 Drill cores

The drill cores (B1–B5/12, see Fig. 2b) analysed for this study were recovered from the Bülach Trough as part of a groundwater exploration study by Dr. von Moos AG (2012) commissioned by the environmental authorities of the Canton of Zurich (Office of Waste, Water, Energy and Air, AWEL). Standard commercial coring equipment with drilling diameters ranging from 322 to 82 mm was used to recover cores from the unconsolidated valley fill reaching depths between 65 and 190 m. After an initial on-site description of all drill cores, ~ 500 m of a total 628 m of drill core were stored for detailed sedimentological analysis. After opening, the cores were photographed and described following the lithofacies approach by Eyles et al. (1983) and recommendations by Evans and Benn (2004).

Additional drillings considered for the valley fill reconstruction in this study are either included in the report by Dr. von Moos AG (2012) or have been published separately (e.g. Haldimann 1978; Freimoser and Locher 1980; Kempf et al. 1986, Wyssling 2008, Graf 2009). The drill cores from the Hardwald site (see Fig. 2c) were recovered as part of an unpublished study by Dr. H. Jäckli AG (2008) and sampled in 2008 for luminescence dating only.

Thin-section samples were taken from representative core intervals using the shielded inner parts of intact drill cores (see Buechi et al. 2017a). The retrieved blocks were then impregnated with an epoxy casting resin, cut to size (30 mm × 50 mm), mounted on glass slides, and ground to 0.03–0.04 mm thickness. The thin-sections were then analysed for their micromorphological properties following the nomenclature of van der Meer and Menzies (2011) and the workflow proposed by Carr (2004).

3.2 Compositional analysis

The bulk composition of the fine-grained fraction < 0.075 mm was measured using the same procedure as described in Buechi et al. (2017b). The bulk samples were analysed for total inorganic carbon (TIC), total carbon (TC), and total sulphur (TS) at a resolution of up to 0.8 cm using a Bruker G4 Icarus elemental analyser. Total organic carbon (TOC) is calculated by subtracting TIC from TC. Based on the assumption that all inorganic carbon (TIC) is bound as calcium carbonate, the CaCO₃ content was calculated by multiplying the TIC by a

stoichiometric factor of 8.33. All the results are reported in weight percent.

The composition of the 20–60 mm fraction in gravels and gravelly diamicts was assessed on 100 clasts per sample following the procedure of Graf (1993, 2009). The abundance of the 12 distinguished clast lithology groups was then used as input for hierarchical cluster analysis (CA) and principle component analysis (PCA) performed in the statistical software *R*. These multivariate statistical methods provide two alternative approaches to assess similarities between the samples. The CA was performed on an Euclidean distance matrix using a minimum variance linkage criterion (Ward's method). This approach links the pair of clusters that lead to a minimum increase in within-cluster variance when merged. Different cluster solutions could then be analysed using the *nbClust* package (Charrad et al. 2014). The PCA transforms the data so that the variability of the data discriminates best along principle components, which can then be plotted in a simple scatter plot. In these biplots similarities result in spatial proximity and the contribution of the input variables, i.e. clast lithology groups, is visualized by arrows (same direction indicates correlation; opposite direction indicates anticorrelation; perpendicular arrows indicate no relation; length of arrow indicates importance of the individual factor). In contrast to CA, the biplots can visualize gradual differences, e.g. mixing effects. Lithology group litho-H1, comprising friable, locally derived silt- and sandstones, was excluded for the CA and PCA due to the random distribution. The data were centered and (log + 1)-scaled to reduce the natural scatter of the data (see Graf 2009).

The distribution of clast shape and rounding is mostly dependent on particle wear during sediment transport and may reveal sedimentary processes and routing in a catchment (e.g. Benn and Ballantyne 1994). Clast shapes were analysed by measuring the clast dimension (a-, b-, c-axis) and rounding was assessed by visual comparison against the rounding chart of Powers (1953). While it is generally recommended to describe clast shape and rounding on only similar lithologies (e.g. Lukas et al. 2013), we used all clasts, independent of lithology (except locally derived friable sandstones). This is because the total number of clasts in the drill core is limited and sampling for specific lithologies would significantly increase the sampling depth interval. The lithology-related bias is, however, relatively moderate as indicated by tests with subsamples. The clast dimensions were plotted in Sneed and Folk (1958) diagrams accompanied by histograms with the clast rounding according to the procedure of Benn and Ballantyne (1993).

3.3 Luminescence dating

Samples for luminescence dating were taken from intact core sections from which the outer, light-exposed parts were removed under subdued red light conditions in the luminescence laboratory at the University of Bern, Switzerland. The samples were then treated with hydrochloric acid (32%) and hydrogen peroxide (30%) to remove carbonates and any organic components, respectively. The fine-grained (4–11 μm) polymineral fraction was then extracted using differential settling in Atterberg cylinders. To obtain the fine-grained quartz fraction, half of the polymineral fraction was etched in H_2SiF_6 for 14 days to digest feldspars. For sample B1–52 it was not possible to isolate a sufficient quartz fraction. From four sandy samples the 200–250 μm coarse-grained fraction was extracted by dry sieving and quartz and K-rich feldspar grains were then density separated using LST Fastfloat heavy liquid at 2.70 and 2.58 g cm^{-3} . The coarse-grained quartz grains were etched with 40% hydrofluoric acid for 1 h. Fluorides were removed from both grain-size fractions by immersion in 32% hydrochloric acid for 1 h. For measurement in the luminescence reader, the aliquots were mounted on stainless steel discs. Fine-grained samples were settled in acetone and coarse grains were fixed using silicone spray.

All measurements were performed on Risø TL/OSL DA-20 readers. Luminescence was stimulated with blue LEDs for 60 s to obtain the quartz OSL signal (Q OSL), and IR LEDs for 300 s to obtain the IRSL₅₀ signal of feldspars. The signals were detected with an EMI 9235QB photo-multiplier tube after passing through 7.5 mm of Hoya U-340 transmission filter for Q OSL, and a 410 nm interference filter and one Schott BG-39, for IRSL₅₀ on feldspar. The determination of the equivalent doses (D_e) were made using modified versions of the single-aliquot regenerative-dose (SAR) protocol (Murray and Wintle 2000; 2003) and benefitted from the detailed characterization of the luminescence properties of drill core B5/12 by Buechi et al. (2017b), where a more detailed account of the measurements is provided.

The natural dose rate was calculated from the concentrations of U, Th, and K (see Supplementary Table 1) as determined for each sample by high-resolution gamma spectroscopy on 400–500 g of bulk material from the surrounding core section (Preusser and Kasper 2001). No evidence was found to suggest radioactive disequilibrium in the Uranium decay chain (Preusser and Degering 2007). The cosmic dose contribution was considered using present-day sample burial depth (Prescott and Hutton 1994). A ^{40}K content for feldspars of $12.5 \pm 0.5\%$ was assumed to estimate the internal dose contribution (Huntley and Baril 1997). The average paleo-water content was estimated as $25 \pm 5\%$ for fine-grained and $20 \pm 5\%$ for coarse-grained samples (see Buechi et al. 2017b).

Fig. 3 a Summary logs of drill cores B1/12–B5/12. Lithofacies codes after Eyles et al. (1983), and Evans and Benn (2004). Clast shape index abbreviations: RWR % ‘rounded’ and ‘well-rounded’ clasts, RA % ‘angular’ and ‘very angular’ clasts; C40 % of platy and elongated clasts. **b** Continued. **c** Continued. **d** Continued. **e** Continued

4 Results

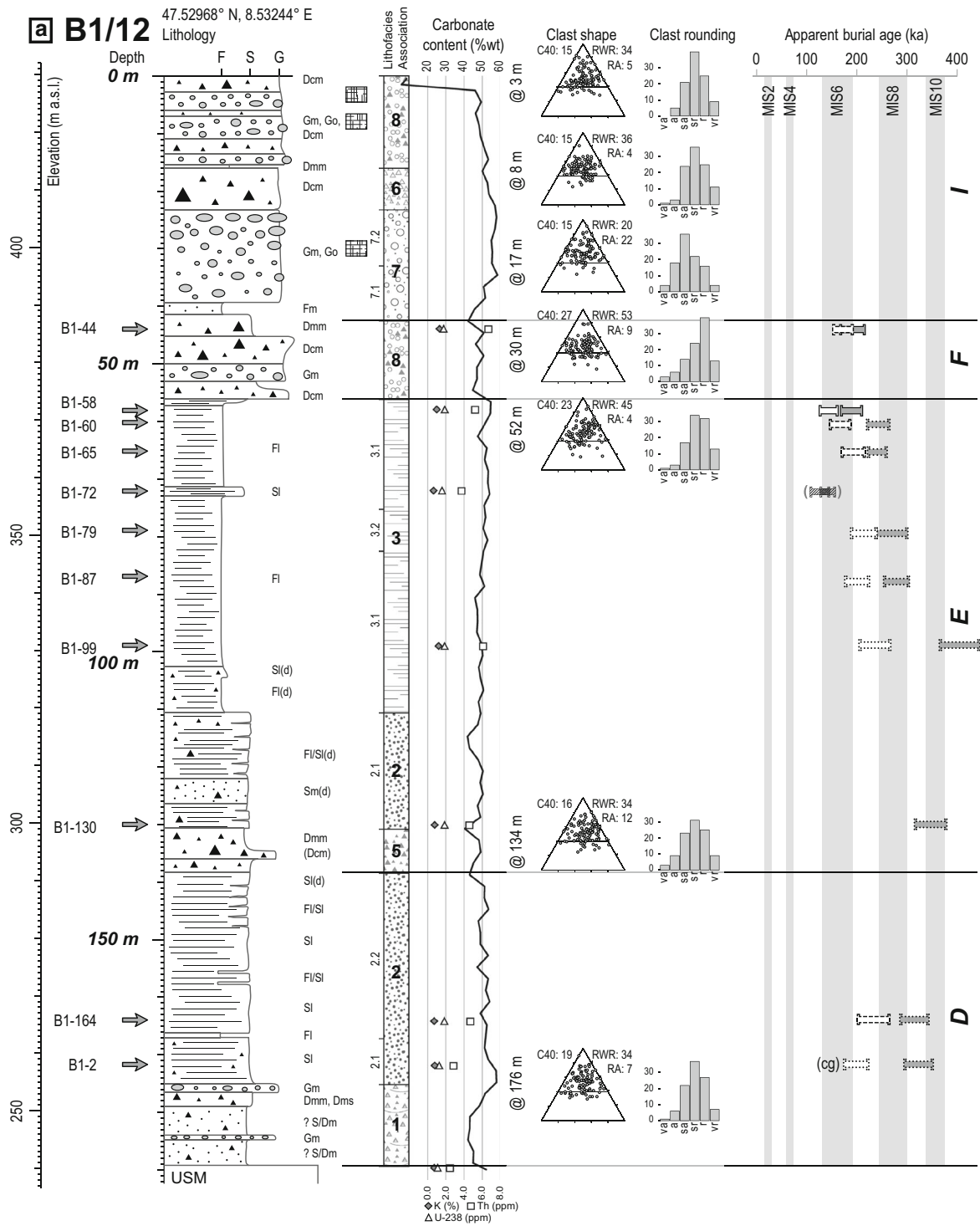
4.1 Lithofacies in drill cores and outcrops

Eight main lithofacies associations (LFA) were identified in the drill cores from the LGV (B1–B5/12, see Fig. 3a–e) and the Hardwald site (B08-4, -5, -7, see Fig. 4). The complete summary description with facies codes (italic below), compositional information, architecture, and micromorphology is provided in Table 1. Figure 5 shows representative core pictures for all LFAs. LFA1–4 are based on Buechi et al. (2017a), who investigated the sedimentary facies of the basal valley fill in the Bülach Trough.

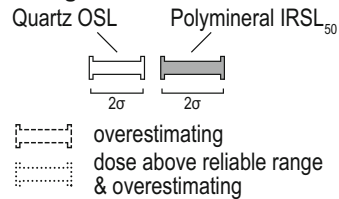
LFA1 comprises densely packed, gravel-rich diamictons (*Dmm*, *Dms*) with sorted waterlain interbeds (*Fl*, *Sl*, *Gm*) and is interpreted as subglacial tills with intervening periods of ice-bed decoupling and subglacial cavity deposition (see Buechi et al. 2017a). The occurrence of *LFA1* is limited to the deepest infill of the bedrock troughs (B1-, B5/12, Fig. 3). Potential equivalents of *LFA1* have been recovered in similar basal position in nearby flushed drillings (e.g. G6, AZ-2; Fig. 2b) and potentially also in the Strassberg Trough (G14, G12, and AZ-4; see Freimoser and Locher 1980; Dr. H. Jäckli AG and DMT GmbH 2012). This correlation is also supported by the hydrogeological properties (see Freimoser and Locher 1980; Buechi et al. 2017a).

The thick fining-upward sequences (*LFA2*) of stratified and massive sands (*Sl*, *Sm*) in the lower portion of the basin fill are interpreted as deposits of glacio-deltaic origin primarily fed by quasi-continuous underflows from the retreating glacier front during deglaciation (see Buechi et al. 2017a). Subfacies *LFA2.1* corresponds to a more ice-proximal, potentially even submarginal, depositional environment additionally influenced by re-sedimentation and dropstones as indicated by interbedded diamictons from subaqueous debris flows and outsized clasts, and may be referred to genetically as waterlain tills (Dreimanis 1979, Schlüchter 1997). *LFA2.2* appears to be slightly more distal, with the latter two depositional processes absent. *LFA2* occurs mostly in the form of thick bodies in the basal Bülach and Strassberg Trough (see B1-, B5/12, Fig. 3 and flush drillings G6, G14; Freimoser and Locher 1980).

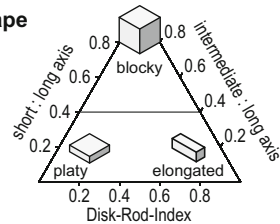
The laminated silt and clay (*Fl*) facies (*LFA3*) dominates the Bülach and Strassberg Trough infill and is interpreted as mainly the result of deposition from turbidity currents and settling from the water column in an ice-



Dating



Clast shape



- Color alteration
- Cemented gravel / clasts with carbonate coatings
- Organic remains

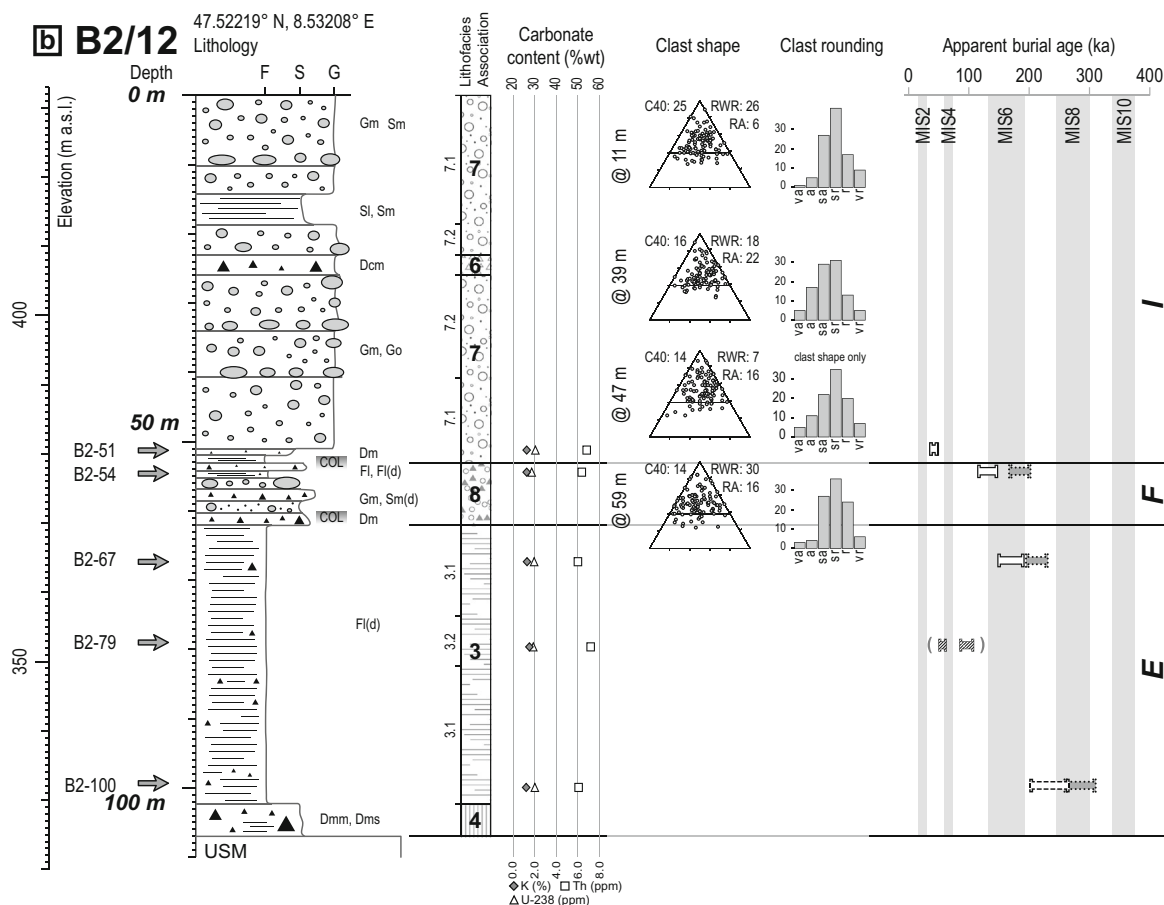


Fig. 3 continued

contact proglacial lake (see Buechi et al. 2017a). In LFA3.1 outsized-clasts interpreted as dropstones and occasional sandy interbeds from outrunning turbidity currents suggest deposition in a glacier-fed lake, whereas during deposition of LFA3.2, the glacier may have been disconnected from the lake as indicated by the better overall sorting and the absence of larger dropstones. The Bülach and Strassberg Troughs are both infilled with tens of meters of LFA3 sediments (e.g. B1-, B5/12 in Fig. 3 and G14, AZ-4, see Freimoser and Locher 1980; Dr. H. Jäckli AG and DMT GmbH 2012). The drill cores from the Hardwald site also recovered LFA3.2 sediments (Fig. 4), which represent the topmost part of a valley infill similarly dominated by LFA3 sediments as in the LGV (Haldimann 1978; Wyssling 2008). In a nearby drill core (~ 1.5 km NW) organics-bearing clays and silts in similar stratigraphic position have been interpreted as interglacial lacustrine sediments (Longo 1978). LFA3 sediments are also observed as several meter thick beds separated from the main valley fill and in a non-overdeepened position (e.g. B3/12: 14–22 m, B5/12: 24–31 m depth, Fig. 3).

The matrix-supported densely-packed diamictons (*Dmm*, *Dms*) of LFA4 are interpreted as subglacial tills.

They are characterized by colourful smears (“marbled” appearance) as well as friable bedrock rafts within the diamict indicating bedrock thrusting, plucking, and limited homogenization of this till type (see Buechi et al. 2017a). LFA4 occurs at the bedrock contact in drill cores B2- to B4/12 (Fig. 3), while it is absent at the bedrock contact in B1/12 in the deep basin, where LFA1 occurs over bedrock instead.

LFA5 comprises dark grey, silt-rich, matrix-supported diamictons (*Dmm*) with occasional clast-supported interbeds (*Dcm*) and is interpreted as subglacial till as indicated by the overall poorly sorted character, the dense packing and consolidation, and the occurrence of glacially striated clasts. Relatively low rounding values may support a glacier-influenced deposition. While similarities with cohesive debris-flow deposits are evident (Menzies and Zaniewski 2003; Phillips 2006), in situ crushed grains observed in thin-sections (Fig. 6a, b) strongly support a subglacial loading and shearing of these sediments (Hooke and Iverson 1995; Hiemstra and van der Meer 1997; Menzies et al. 2006; Buechi et al. 2017a). This interpretation is further supported by the occurrence of (1) turbate features indicating ductile rotational deformation or turbulence

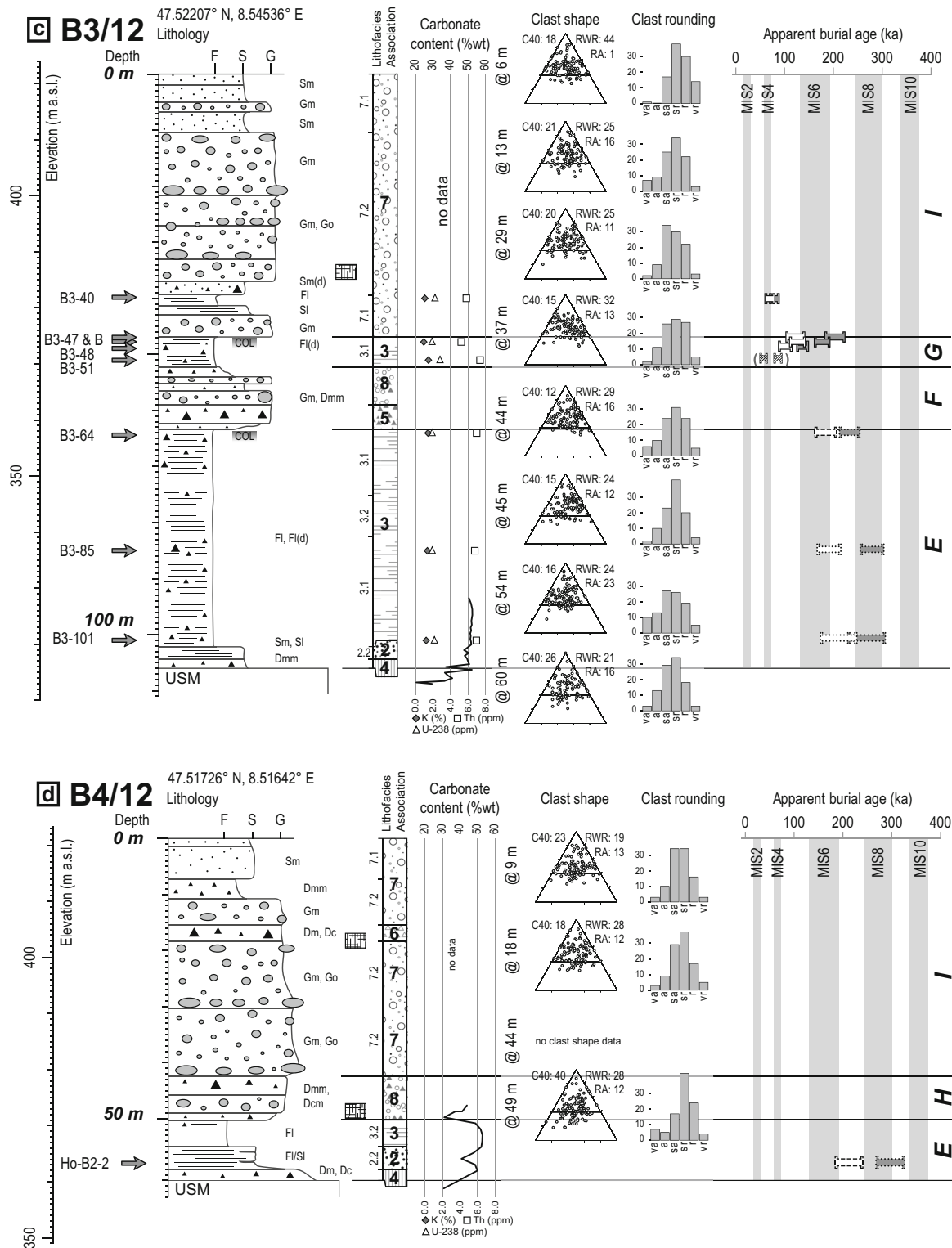


Fig. 3 continued

(Menzies 2000; Hiemstra and Rijdsdijk 2003; Phillips 2006) and (2) lineations representing microshears that probably evolved in response to local syn-depositional and post-depositional stress alterations (Menzies et al. 2006;

Menzies and Ellwanger 2011). Despite careful sample selection, a drilling-related component of these deformations cannot be fully excluded, particularly the longer lineations in Fig. 6d could be related to drilling disturbance

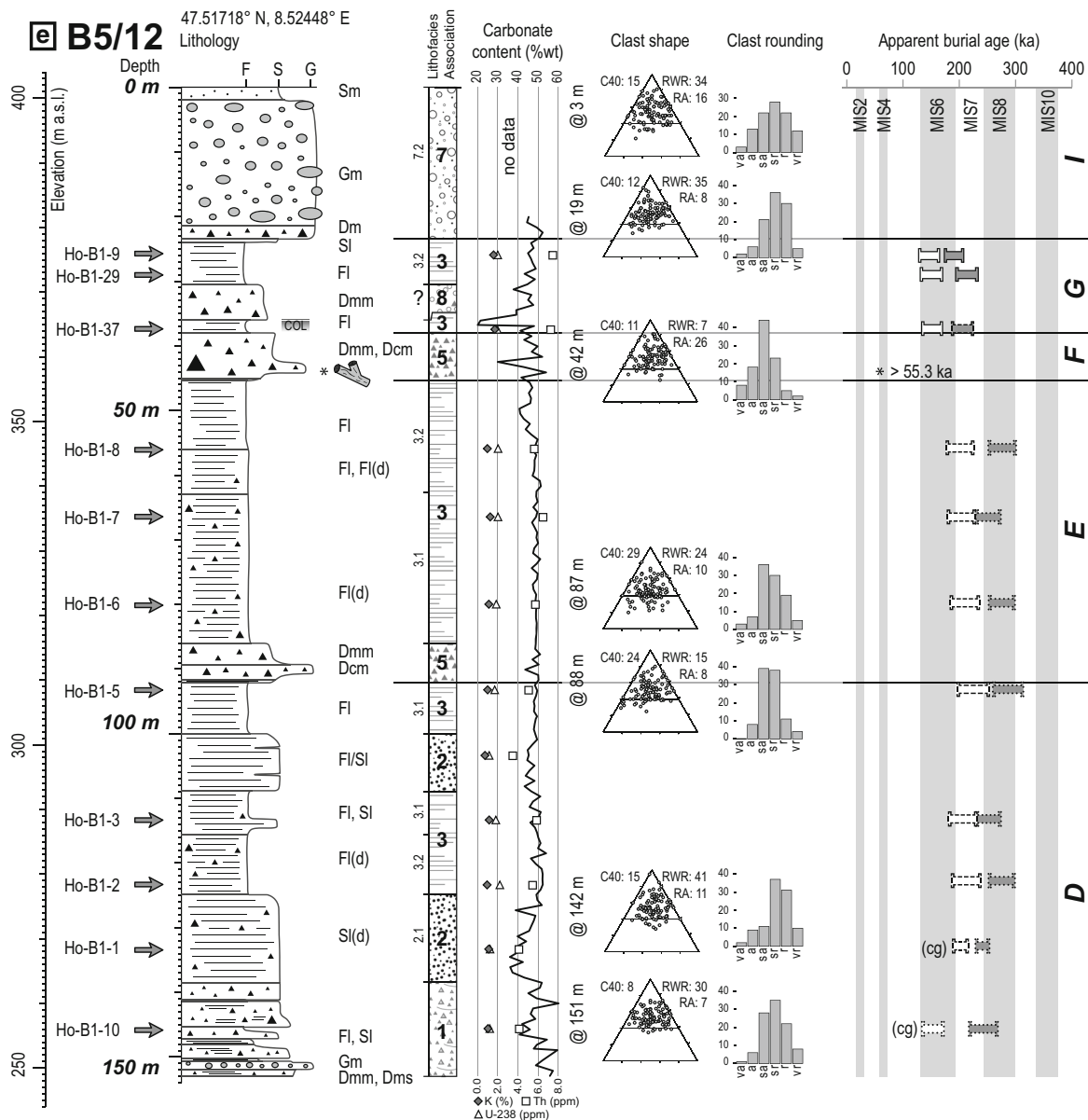


Fig. 3 continued

(Carr 2004). The dark-colour and fine-grained character of the matrix is interpreted as resulting from reworking of glacio-lacustrine deposits (mainly LFA3), which underlie LFA5 in all observations (see B1-, B3-, B5/12, Fig. 3). This interpretation is in agreement with Schlüchter (1977), who ascribed the excess of fine-grained components in ‘mud tills’ to the reworking of glacio-lacustrine sediments. Such reworking is also indicated by the occurrence of clay-coated grains, which are probably derived from the underlying LFA3, and incorporated in the subglacial till (Fig. 6b, d). Ample soft-sediment deformation features of the fine-grained lacustrine deposits documented at the basal contact (Fig. 6c, d) likely document subglacial deformation by glacial overriding.

LFA6 consists of clast-supported, gravely diamictos (*Dcm*) with a sand- and silt-rich matrix with occasional matrix-supported intervals (*Dmm*). These deposits are interpreted as subglacial tills as indicated by the densely packed, consolidated character of these diamictos, the occurrence of glacially overprinted clast shapes, and glacial striations. In gravely sediments, diamictic segments of similar appearance as subglacial tills may be produced during drilling. Such spurious intervals (typically less thick than LFA6 beds, occurring towards the end of a drilling run, or occasional occurrence regarding surrounding drill cores) were not included in LFA6. Additional investigations of the plasticity of the fine-fraction may help to better distinguish these drilling-related diamictos but were,

Table 1 continued

Lithofacies Association	Architecture		Occurrence in formations (Fm) and relation to other LFAs	Basal contact	Micromorphological summary description	Genetic interpretation
	Typ. thickness (in m)					
LFA1 Diamicts with sorted interbeds	LFA1.1 LFA1.2 LFA1.3	1–4 1–1.5 0.1–0.5	<i>Fm-D (Fm-B?)</i> Overlying bedrock in the deep bedrock troughs Stacking of diamicts (LFA1.1) with thin sorted interbeds (LFA1.2 and 1.3)	Sharp Sharp Sharp	Abundant polyphase deformation features, abundant in situ grain-crushing – Deformed depositional banding, abundant polyphase deformation features, in situ grain-crushing absent	Subglacial till, subglacial cavity fills
LFA2 Stratified sands	LFA2.1 LFA2.2	5–15 10–30	<i>Fm-B, -D and -E</i> Thick infill in bedrock troughs, underlain by bedrock or LFA1. LFA2.1 and 2.2 typic. in vertical succession and/or interfingering	Gradual or sharp Gradual or sharp	Minor post-depositional deformation, planar- to cross-bedding	Proximal basin-floor fan with reworking Distal basin-floor fan
LFA3 Laminated silt and clay	LFA3.1 LFA3.2	10–35 10–20	<i>Fm-B, -D, -E, -G</i> Thick infill in bedrock troughs, underlain by bedrock or LFA2 LFA3.1 and 3.2 typic. in vertical succession and/or interfingering	Gradual Gradual	Minor post-depositional deformation, planar- to cross-bedding	Proglacial lake deposits, strong glacier influence Glacier distal lake deposits, weak glacier influence
LFA4 “Marbled” diamicts	LFA4	2–5	<i>Fm-E (Fm-B, -D?)</i> Overlying bedrock on trough shoulders Overlain by LFA2 and -3	Gradual	–	Subglacial till, glacio-tectonized bedrock
LFA5 Matrix-rich diamicts	LFA5	4–8	<i>Fm-E and -F</i> Diamictons truncating fine-grained valley fill LFA3 (and -2)	Sharp or narrow transition zone	Abundant polyphase deformation features, abundant in situ grain-crushing, narrow deformation zone at contact with LFA2	Subglacial till strongly influenced by reworking of fine-grained valley fill (mostly in association with LFA2 and 3)

Table 1 continued

Lithofacies Association	Architecture		Occurrence in formations (Fm) and relation to other LFAs	Basal contact	Micromorphological summary description	Genetic interpretation
	Typ. thickness (in m)					
LFA6 Gravel-rich diamicts	3–7 m	<i>Fm-I</i>	Diamictons in close association with LFA7 and -8	Gradual (poor recovery)	–	Subglacial till strongly influenced by reworking of gravelly valley fill (mostly in association with LFA7)
LFA7 Gravels	LFA7.1 7–20 LFA7.2 15–30	<i>Fm-A, -C, H and -I</i>	Limited to non-overdeepened positions, LFA7.2 and 7.1 typic. in vertical succession and/or interfingering In correlated outcrops planar- to cross-bedded	Gradual or sharp Gradual or sharp	–	Distal fluvio-glacial to fluvial outwash Fluvioglacial outwash, more proximal than 7.1
LFA8 Gravels w/Interbedded diamicts	7–17	<i>Fm-F and -I</i>	Close association with LFA5,6, 7	Gradual or sharp	–	Alteration between fluvial and mass-wasting processes in ice-marginal and fluvial channel settings

C40 = % clasts with short-axis/long-axis ratio of > 0.4; RA = % angular and very angular clasts; RWR = % rounded to well-rounded clasts

^a Clast shape determined on 100 clasts per sample

^b 0: no finds, +: rare finds (0–3), ++: several finds (3–10)

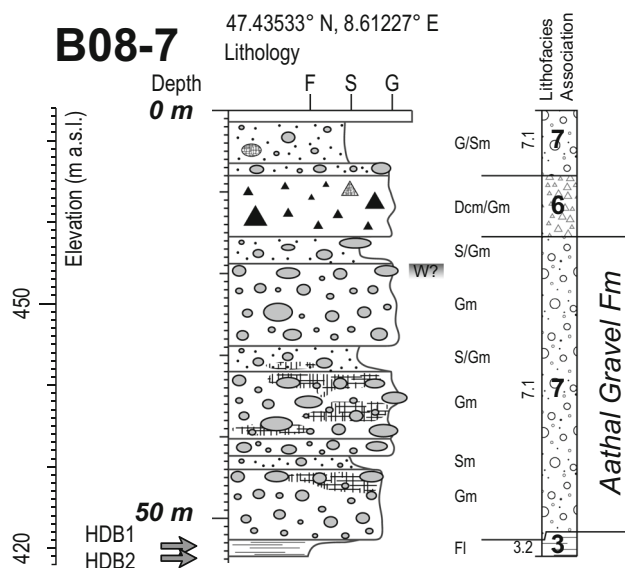


Fig. 4 Summary log of drill core B08-7, which is representative for the two additional drill cores from the Hardwald site (B08-4, B08-5). Lithofacies codes after Eyles et al. (1983), and Evans and Benn (2004). Luminescence dating samples HDB3-4 were taken from the same stratigraphic position as HDB1-2

however, not tested (e.g. Boulton and Paul 1976; Schlüchter 1997). The gravel-rich character of LFA6 is interpreted as resulting from subglacial re-working of gravelly sediments (LFA7) with which it is closely associated. However, compared to other gravelly facies (LFA7), the proportion of angular clasts is higher, and that of rounded clasts lower, indicating glacier overprint during re-working (see RA, RWR, Table 1). LFA6 tills were recovered in the upper parts of the valley fill in drill cores B1-, B2-, B4/12 (Fig. 3) and make up the sediment of the terminal moraine complex (Fig. 2), which supports our sedimentological interpretation. At the Hardwald site these sediments have been interpreted similarly as till cover (Dr. H. Jäckli AG 2008).

LFA7 consists of thick-bedded gravels interpreted as fluvial and fluvio-glacial deposits of a proglacial outwash plain as suggested by the occurrence of boulder-sized clasts, rare glacially shaped clasts, and the thick-bedded aggradational nature of these units. Subfacies LFA7.1 includes sorted gravels (*Gm*, *Gc*) with clasts up to ~ 15 cm length and occasional fine-grained interbeds (*Sm*, *Fl*). Unidentified gastropod shells found in a fine-grained sandy interbed at the Hardwald site (core B08-04 at ~ 28 m depth) may indicate a fluvial plain with stable, habitable river banks or backwater areas. Subfacies LFA7.2 comprises the less sorted gravel units (*Gm*, *Dcm*) with a variable silt and sand matrix, which suggests that LFA7.2 gravels represent the more glacier proximal sediments that underwent shorter fluvial transport than LFA7.1. Coarse gravel and boulder layers (*Gm*, *B*) overlain by crude fining-

upward sequences spanning over several meters are interpreted as erosional and aggradation cycles within the outwash plain dynamics (e.g. Maizels 1993; Siegenthaler and Huguenberger 1993). LFA7 is the dominant lithofacies in the upper valley-fill and occurs in all drill cores and at various outcrops (e.g. outcrops at Chatzenstig and Oberschwendli, Fig. 7, and near Herrenwies, Fig. 8).

LFA8 consists of poorly sorted gravels (*Gm*) frequently interbedded with gravel- and sand-rich diamicts (*Dcm*, *Dmm*). This facies is interpreted as an alternation between sorted fluvial deposition, indicated by similar clast shape and rounding as in LFA7, and unsorted mass-wasting deposition, e.g. cohesive debris-flows, indicated by matrix-agglomerated core pieces. LFA8 sediments have been recovered in a variety of stratigraphic contexts, indicating that deposition may occur in different environments. LFA8 primarily appears to be closely associated with tills and may represent ice-marginal sedimentation. In this setting, the stacking of diamicts and gravels is likely to represent the alternation between glacial tills (submarginal and supra-glacial), debris flows, and sorted deposition by meltwater. This is well-documented in core B1/12 (0–16 m depth, see Fig. 3a), where LFA8 overlies an LFA6 till that can be tied to a terminal moraine and where reworked glacially shaped clasts, indicated by striations, and bullet- and flat-iron-shapes, are relatively common. Alternatively, similar sediments may be deposited where sorted sedimentation is influenced by occasional mass-wasting from unstable debris slopes such as deltaic settings or slope instabilities along incising fluvial channels. Such a setting would explain the occurrence of LFA8 at the transition from lacustrine (LFA3) to gravelly deposition (LFA7) in drill cores B1-, B2-, and B4/12, or interbedded into a shallow lacustrine sequence (B5/12 at 31–36 m, for all see Fig. 3).

4.2 Clast lithological analysis (20–60 mm)

The lithological composition of the sampled core section (Table 2) is dominated by limestones (Litho-A to -D) with an average of $52 \pm 6\%$ per sample. Frequent constituents are further quartzites (Litho-I, $17 \pm 4\%$), Alpine sandstones (Litho-H2, $14 \pm 4\%$), and hornfels/chert (Litho-K, $7 \pm 3\%$). The remaining clast lithology groups (Litho-F, -G, -L, -M) remain generally rare or absent, but higher counts are observed in some of the samples. These results are in good agreement with previous studies, which confirm very similar compositions of the Middle to Late Pleistocene gravel units in the Lower Glatt valley (Zingg 1935; Graf 2009). Indicator lithologies of the Linth-Rhein-Glacier are quartzites, schists, and volcanic lithologies from the Glarus Verrucano Basin unit (e.g. Trümpy and Dössegger 1973; Hantke 1978; Zhang et al. 1981; Letsch



Fig. 5 Representative core images of the lithofacies associations LFA1-8 and bedrock

et al. 2015). These lithologies occur throughout all samples but remain rare and could not be represented in a separate lithology group given the chosen sample size. Local sandstones (Litho-H1) are only occur as individual finds.

The dendrogram resulting from hierarchical clustering of the clast lithology samples (Fig. 9a) is shown with a three-cluster solution, which is suggested as the best clustering scheme by a majority of clustering validity indices (Charrad et al. 2014). Cluster Clu-1 indicates a very similar composition for all samples from LFA1 (see also Buechi et al. 2017a). Clusters Clu-2 and -3 comprise a wide range of samples without a clear correlation to position of the samples in the drill core (stratigraphic order) or to lithofacies (represented by the symbols).

Better insight into the total composition and sample relationship is provided by the PCA biplot (Fig. 9b) documenting that, overall, samples are well-spread and distinct clustering is not apparent. Litho-B and -D (black and other

limestones) are positively correlated, but anti-correlated with groups Litho-M (granitic, metamorphic and igneous lithologies) and Litho-L (vein quartz). The first principle component broadly follows the axis connecting these two poles. Lithological groups Litho-H2 (Alpine sandstones), -K (chert, radiolarites) and -F (dolomites) are also positively correlated, but are anti-correlated with groups Litho-A (dark grey limestones) and -I (quartzites) and strongly discriminate along the second principle component.

In the biplot, the samples are further coded as tills (triangles; LFA1, 5, 6), fluvial gravels (circles; LFA7) and interbedded gravels and diamicts (rectangles; LFA8). The till samples can be generally discriminated from the other samples due to a higher abundance of crystalline components (Litho-L, -M), Alpine sandstones and hornfels/chert (Litho-H2, -K), dolomites (-F), and subalpine sandstones (-G). The overall more colourful spectrum of lithologies in the till samples is likely to represent direct sediment

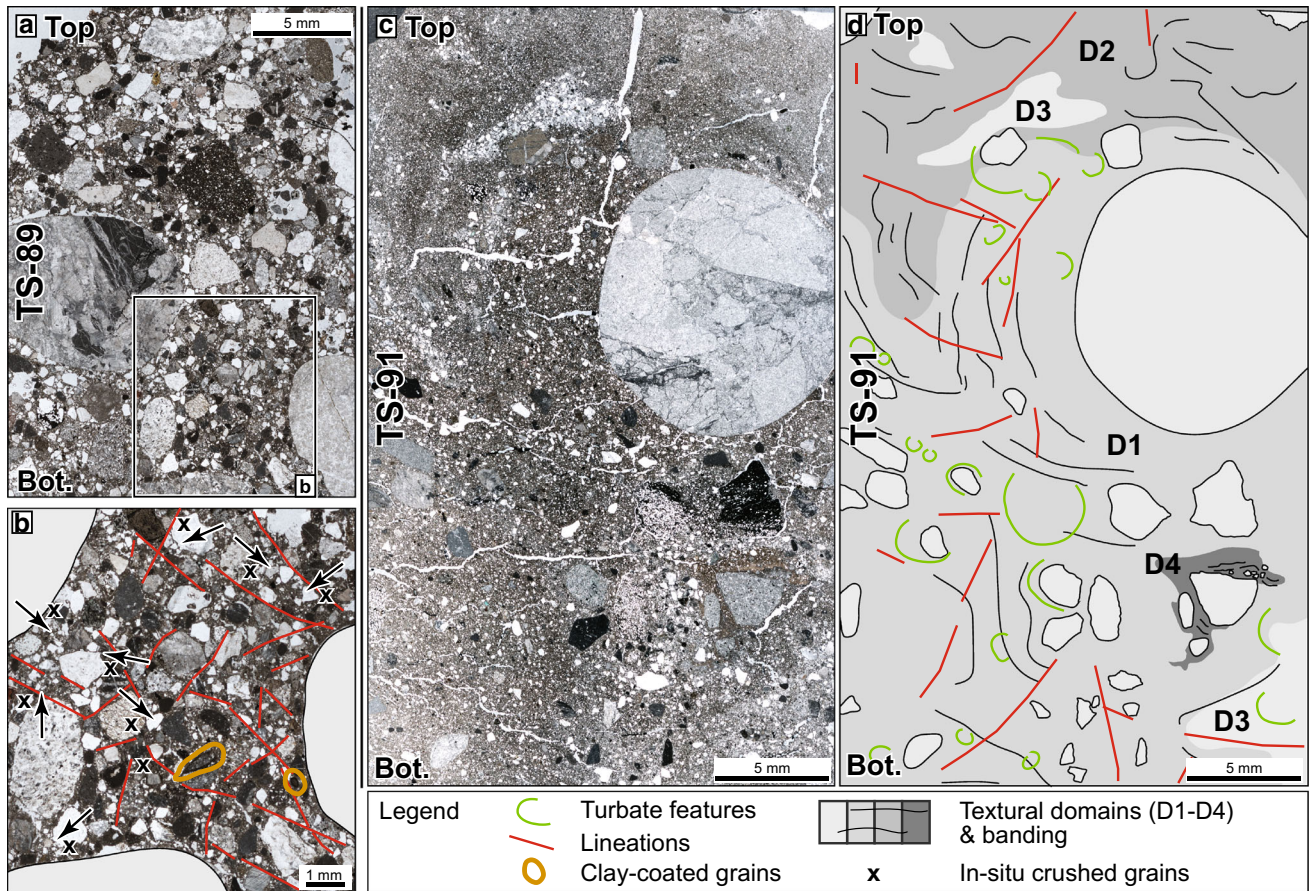


Fig. 6 Thin-section of the LFA5 diamicton in core B5/12. **a** At 89 m depth, a relative sandy interval reveals a densely-packed diamicton supported by sand-sized grains up to ~ 10 mm in diameter. A wide-spectrum of grain shapes from well-rounded to angular can be observed. Grains with mixed, rounded and angular, outline parts are common. **b** In close-up view many grains are crushed and appear as separated pieces and flakes close to the main grain. These in situ crushed grains are typical for high stress concentrations attained at grain contacts during subglacial deformation. Microstructural

delivery from the Alpine catchment or from the Molasse conglomerates in the upper Glatt valley and/or the lower resistance of some of these lithologies to fluvial transport (e.g. Molasse-derived granites, see also Zingg 1935). Samples from LFA7 and 8 tend to be centered in the upper half, but with a considerable spread over the entire biplot.

These results thus suggest that the lithological composition of the samples is relatively constant through a wide range of lithofacies and potential stratigraphic levels in the LGV drill cores. This interpretation is founded on the occurrence of Linth-Rhein Glacier indicator lithologies, similar proportions of the major components (Litho-A to -D, -H2, -I, -K), and small standard deviations when all samples are compared. Observed compositional differences are graduated between the samples as indicated by the relatively large scatter and absence of distinct clustering in the biplot. Overall, the gravel composition therefore is interpreted to reflect a generally

mapping further reveals the common occurrence of mm-long lineations throughout the sediment. **c** Thin-section taken from the transition between LFA5 till and glacio-lacustrine sediments (LFA3) at 91 m in B5/12. Texturally similar regions (domains D1–D4), probably reflecting initial sedimentary structures, and accessory turbate features, with tangentially aligned clast long-axis, appear to be contorted around the larger grain at the centre of the thin-section potentially in response to subglacial deformation

constant sediment source and transport path, and/or a significant amount of reworking (see also Zingg 1935).

4.3 Bulk composition (< 0.075 mm)

The bulk carbonate content of the fine fraction (< 0.075 mm) is relatively constant with values of ~ 40 – 55% throughout most of the drill cores (see drill core logs in Fig. 3 and Table 1). The variation between samples is in the range of a few percent for the fine-grained lithofacies (LFA3), while this range is up to 10% for gravelly and diamictic lithofacies. Lower values occur (1) in the USM bedrock (as low as 20%), (2) the directly overlying diamictic and sandy lithofacies in the lowermost valley fill (as low as 35%, LFA1, 2, 4, see Buechi et al. 2017a), and (3) in B5/12 at 36 m depth ($\sim 21\%$). The strongest depression is observed in the top 1.5 m of B1/12

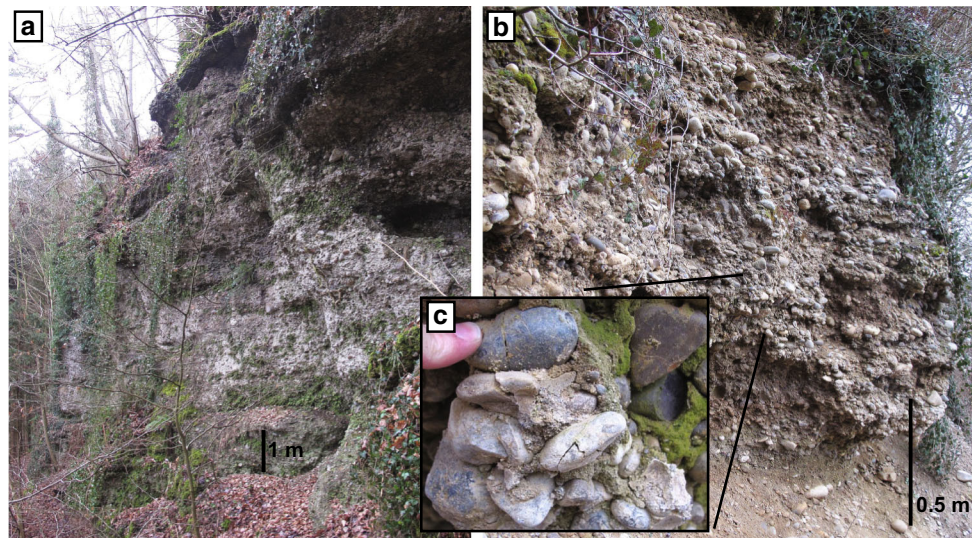


Fig. 7 Outcrops of fluvial or distal fluvio-glacial gravels (LFA7.1). **a** Planar-bedded gravels along the north-eastern edge of the Strassberg Plateau (outcrop B in Fig. 2a) with strong surface cementation.

b Weathered gravels at the Oberschwendli outcrop (outcrop C in Fig. 2a). **c** Broken clasts (example from Oberschwendli) can be found in both outcrops. Both outcrops are correlated to Formation C

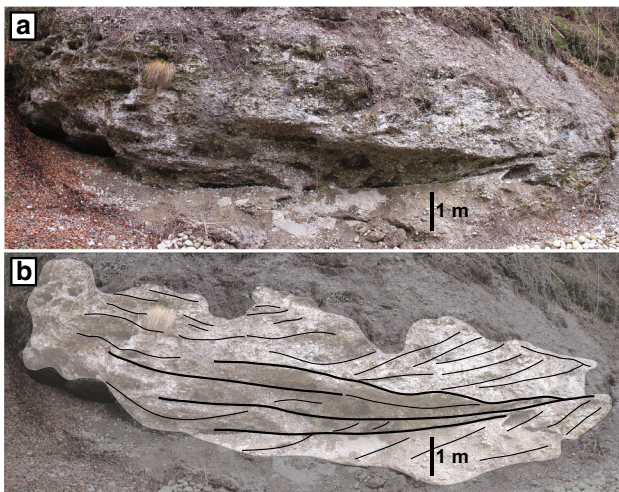


Fig. 8 Outcrop at Herrenwies with cross-bedded fluvial gravels (LFA7.1, internal stratification indicated in **b**) interpreted as channel or scour-pool fills deposited in a glacial outwash plain. These gravels are correlated to Formation I. For location see Fig. 2a, label D

with carbonate contents of 6-8%, which reflects decalcification due to modern soil formation on this surface.

The characteristic carbonate contents of $\sim 50\%$ in the valley fill is higher than in typical bedrock in the LGV and must therefore be sourced from either the inner-Alpine carbonate-rich glacial catchment (mostly Helvetic nappes) and/or from the carbonate-rich Molasse in the Upper Glatt valley (mainly Upper Freshwater Molasse of the Hörnli Fan). Similar carbonate contents have been reported from the drill cores into the Quaternary valley fill in the

neighbouring Wehntal (Anselmetti et al. 2010; Dehnert et al. 2012). A marked decrease in the carbonate content in the upper ~ 17 m of these two drill cores was interpreted as representing the cessation of carbonate-rich silt delivery to the Wehntal in response to glacier retreat. It was argued that such a disconnection could have occurred during retreat of the glacier behind the bedrock sills at the entrance of the Wehntal or at Hombrechtikon. Such a sudden reduction in the carbonate content is, however, not observed in the Lower Glatt valley. While this section may simply have been eroded, the continuously high carbonate content in the LGV in all sites may instead be the expression of continued carbonate-rich sediment delivery to the LGV. In the latter case, the carbonate may be brought in either from reworking of glacial sediments or carbonate-rich Molasse bedrock in the Upper Glatt valley.

The total organic carbon (TOC) and total sulphur (TS) contents amount to $\leq 0.5\%$, and thus generally below the detection limit of the applied method. In B1/12, an individual measurement yielded slightly increased TS (0.16%, 22.5 m) and TOC (1.8% at 42.5 m depth) values. These results suggest limited organic input or production and/or poor preservation in the valley fill. Low organic production is in broad agreement with the interpretation of the different lithofacies in a glacial and proglacial environment under cold climatic conditions. The low preservation potential of warmer-period deposits along the main valley axis is interpreted as resulting from the exposure of interglacial or interstadial organic-rich layers to fluvial and glacial erosion with the onset of the subsequent glaciation.

Table 2 Clast counting results grouped into lithological groups

Samples	Litho-A	Litho-B	Litho-C	Litho-D	Litho-F	Litho-G	Litho-H1	Litho-H2	Litho-I	Litho-K	Litho-L	Litho-M	Broken clasts	Glacial striations	Flat-iron-, bullet- and arrow-shaped clasts	Carbonate cements/ weathered clasts (w)
B1-3	16	19	3	21	1	1	0	20	10	4	3	2	+	++	+	++
B1-8	19	11	6	19	3	1	1	15	12	8	1	4	+	++	-	++
B1-17	15	18	5	14	2	1	1	14	17	5	5	3	++	-	+	-
B1-30	10	16	5	12	3	2	0	16	18	10	3	5	+	-	-	++
B1-52	23	13	8	9	1	0	0	20	10	9	2	5	+	-	-	-
B1-134	13	9	6	16	3	4	0	21	13	6	3	6	+++	-	-	-
B1-176	19	6	7	15	6	1	0	15	14	7	2	8	+	-	-	-
B2-11	30	6	6	18	0	0	1	12	16	5	4	2	+	+	-	-
B2-39	19	16	3	16	0	1	0	14	18	6	2	5	+++	+	-	-
B2-59	20	15	2	16	0	1	1	11	22	9	1	2	+++	-	-	-
B3-6	19	9	6	22	1	1	0	8	21	2	4	7	+	-	+	-
B3-29	13	11	8	12	0	1	0	16	18	13	3	5	+++	-	-	-
B3-37	17	9	4	19	1	2	0	11	23	6	2	6	+++	-	+	+
B3-43	19	11	2	22	2	3	1	10	22	5	2	1	+	-	+	-
B3-46	15	16	8	22	2	1	0	12	17	4	2	1	+	+	-	-
B3-55	13	17	7	18	2	1	2	8	17	3	3	9	+	-	++	-
B3-61	16	8	7	25	0	4	0	13	16	7	0	4	+++	+	++	-
B4-9	12	21	4	19	2	4	0	12	15	8	1	2	+++	-	+	-
B4-18	13	11	2	14	7	0	0	10	23	14	3	3	+	-	+	+
B4-44	17	8	11	14	1	0	0	8	23	6	2	10	+++	-	-	-
B4-49	15	7	2	16	0	2	0	19	15	6	6	12	+	-	-	+, w
B5-3	17	13	11	10	0	1	0	11	22	3	6	6	+++	-	-	-
B5-19	17	9	6	21	1	2	0	15	13	7	2	7	+++	-	-	-
B5-42	14	5	6	17	2	1	3	17	14	8	5	8	+++	-	-	-
B5-87	19	12	7	15	1	1	1	15	16	9	1	3	+	-	-	-
B5-88	13	6	5	13	2	0	1	23	15	12	6	4	+	-	-	-
B5-142	16	9	1	16	9	3	0	13	19	5	3	6	+	-	-	-
B5-151	11	7	4	16	8	1	0	13	18	10	3	9	+++	-	-	-

Litho-A dark-grey limestone, *Litho-B* black limestone, *Litho-C* siliceous limestone, *Litho-D* other limestones, *Litho-F* dolomites, *Litho-G* hard, mica-rich sandstones (sub-Alpine Molasse), *Litho-H1* friable sandstone, mica-rich, friable (local Molasse origin), *Litho-H2* other sandstones (non-local, Alpine catchment), *Litho-I* quartzite, *K* chert, hornfels, radiolarite, *Litho-L* vein quartz, *Litho-M* granitic, metamorphic and igneous rocks

Abundance of striated, glacially shaped clasts, and carbonate coating is coded as follows: "0" no finds, "+": rare finds (0-3), "++": several finds (3-10)

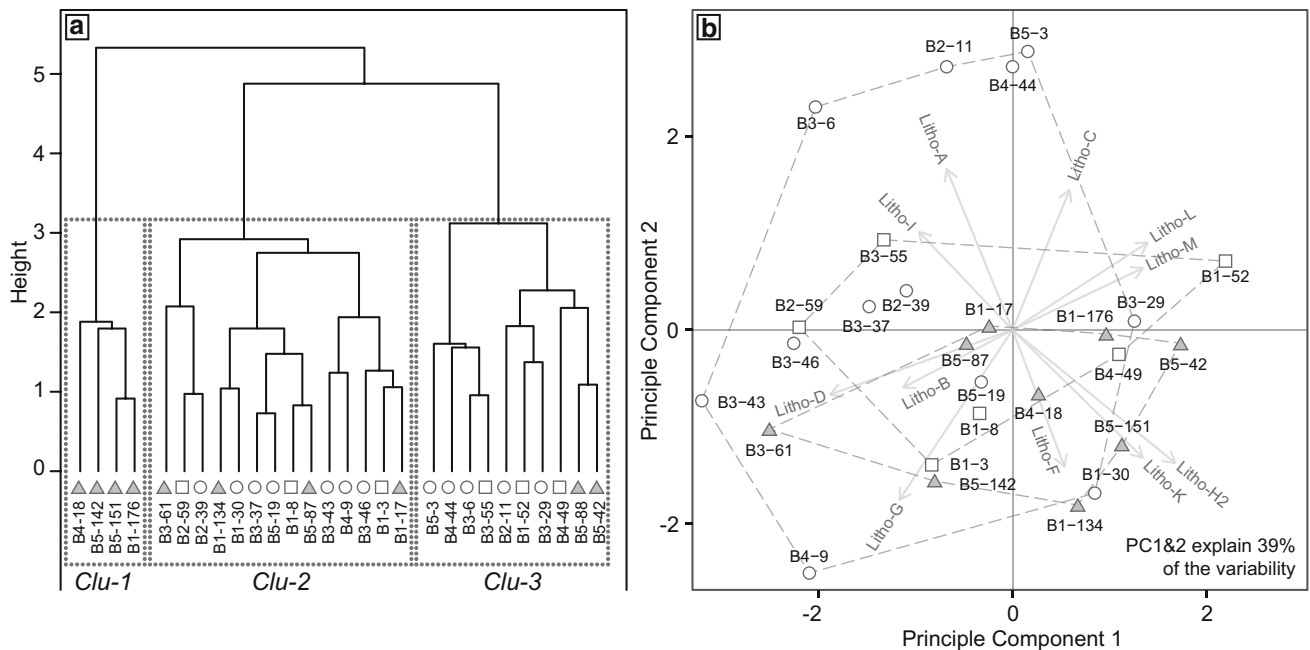


Fig. 9 Cluster analysis dendrogram and PCA biplot of the clast lithological data (see Table 2). For stratigraphic position of the samples see Fig. 3. Symbol shapes indicate different lithofacies: triangles for samples from LFA1, 5, and 6 (tills); circles for LFA7 (fluvial–fluvioglacial gravels); rectangles for LFA8 (interbedded gravels and diamicts)

4.4 Weathering and broken clasts

Apart from soil formation below present-day surfaces (e.g. decalcification in B1/12, Fig. 3a), weathering appears to be more pronounced in the gravel of the Oberschwendli outcrop (see Fig. 7b). Clear evidence for buried weathering surfaces, potentially indicating paleosols, are also found in drill core B4/12 at 49 m depth, where dissolution and oxidation features occur on many clasts along with crumbling sandstone and granite clasts. Similar buried features have been reported from drill core G5 (reported in Dr. von Moos AG 2012).

Light to dark brown and rare greenish mottled colour alterations (typically less than 10 cm thick) also occur at transitions from laminated silts (LFA3) to gravel and diamicts at several locations (e.g. B2/12 at 52 m, B3/12 at 47 and 63 m, B5/12 at 36 m). While similar features may result from soil formation (see above), a groundwater-related chemical alteration related to relatively oxygen-rich groundwaters is preferred for these thin intervals as it would be difficult to explain a surface exposure of most of the coloured lacustrine sediments (e.g. in B5/12). In addition, bulk geochemistry of these layers indicates only partial decalcification and no organic carbon, neither of which would be expected in a soil profile.

Furthermore, mechanically broken clasts, interpreted to result from glacier overriding and related ice load (e.g. Graf and Hofmann 2000), are found in the Chatzenstig and Oberschwendli outcrops (Fig. 7c), where the fractures are

often healed by secondary cements. In clast samples from drill cores, the abundance of broken clasts (Table 2, mostly LFA6, 7, 8) may similarly represent glacier overriding, however, the depositional and deformational context is not as well constrained.

4.5 Dating results

Luminescence dating of the (glacio-)lacustrine sediments recovered in drill cores from the Lower and Middle Glatt valley (see Fig. 1) yielded a coherent set of ages. Dose rates, burial doses, and ages are listed in Table 3 and illustrated in the core logs (Fig. 3). For completeness, Table 3 also includes the results of drill core B5/12 presented in the methodological study by Buechi et al. (2017b).

The burial ages can be divided into three types (type 1-3, in Table 3 indicated by bold numbers, * and ** respectively). Type 1 summarizes the ages that can be considered as reliable estimates of burial age with doses below saturation, i.e. < 400 Gy for fine-grained Q OSL and < 470 Gy for fine-grained IRSL₅₀ according to Buechi et al. (2017b). These samples range between 41 ± 5 and 170 ± 20 ka for Q OSL and 44 ± 4 and 184 ± 15 ka for IRSL₅₀. Where type 1 Q OSL and IRSL₅₀ ages overlap, the samples can be considered well-bleached (e.g. Murray et al. 2012; Dehnert et al. 2012).

Type 2 samples are interpreted as suffering from significant incomplete bleaching and/or reworking of

Table 3 Equivalent doses (D_e), dose rates (D_r), and ages for all samples

Core	Depth (m)	Sample	Fraction (μm)	W_e (%)	Polym mineral fraction (K-Feldspar for coarse-grained samples)		Quartz fraction		Comments										
					D_r (Gy/ka)	\pm	$n_{\text{acc}}/n_{\text{tot}}$	D_e (Gy)	Age (ka)	\pm	$n_{\text{acc}}/n_{\text{tot}}$	D_e (Gy)	Age (ka)	\pm					
<i>Lower Glatt valley</i>																			
B1/12	44.00	B1-44	11-25	20 \pm 5	2.19	0.17	5/5	419	40	191	23	2.07	0.21	5/5	359	15	173	19	Lens of fines (LFA3) in LFA8
	58.00	B1-58	4-11	25 \pm 5	1.74	0.14	5/5	330	23	190	20	1.65	0.19	5/5	238	7	144	17	
	60.40	B1-60	4-11	25 \pm 5	2.26	0.18	3/3	550	21	243**	21	2.16	0.24	4/5	360	9	167	19	
	65.30	B1-65	4-11	25 \pm 5	2.17	0.16	3/3	525	3	242**	18	1.98	0.22	5/5	383	12	193*	22	
	72.25	B1-72	4-11	25 \pm 5	1.32	0.11	5/5	(188)	10	143	14	1.24	0.15	4/5	157	10	126	17	IRSL not considered
	79.50	B1-79	4-11	25 \pm 5	2.27	0.17	3/3	612	52	269**	31	2.17	0.24	5/5	467	15	215**	25	
	87.70	B1-87	4-11	25 \pm 5	2.26	0.17	3/3	631	24	280**	23	2.16	0.24	5/5	433	9	201**	22	
	99.00	B1-99	4-11	25 \pm 5	2.05	0.16	3/5	830	46	405**	38	1.95	0.22	5/5	461	28	236**	30	
	130.00	B1-130	4-11	25 \pm 5	1.57	0.13	9/10	545	13	348**	30	1.48	0.18	-	-	-	-	-	No Q left after etching
	164.00	B1-164	4-11	25 \pm 5	1.55	0.13	9/10	488	6	315**	27	1.46	0.19	10/10	342	11	234*	31	
	171.80	B1-2	200-250	20 \pm 5	1.80	0.13	10/12	582	26	324	27	0.96	0.05	20/24	191	20	199*	23	KFS: $n_{\text{sat}} = 1$, OD = 12; Q: $n_{\text{sat}} = 1$, OD = 45;
B2/12	51.30	B2-51	4-11	25 \pm 5	2.19	0.18	5/5	96	2	44	4	2.09	0.24	4/4	85	1	41	5	
	54.50	B2-54	4-11	25 \pm 5	2.13	0.17	5/5	393	6	184	15	2.04	0.23	4/4	267	6	131	15	
	67.40	B2-67	4-11	25 \pm 5	2.09	0.16	5/5	445	2	213*	16	2.00	0.22	3/4	340	15	170	20	
	79.70	B2-79	4-11	25 \pm 5	2.42	0.18	9/9	(137)	2	56	4	2.32	0.25	4/4	(221)	6	96	10	Not considered
	100.00	B2-100	4-11	25 \pm 5	2.07	0.16	5/5	586	17	284**	24	1.97	0.22	4/4	461	32	234**	31	
B3/12	40.00	B3-40	4-11	25 \pm 5	1.89	0.15	5/5	154	3	82	7	1.80	0.20	7/8	127	7	71	9	
	47.10	B3-47B	4-11	25 \pm 5	2.36	0.19	3/3	480	19	203**	18	2.25	0.26	4/4	273	19	121	17	
	47.80	B3-47	4-11	25 \pm 5	1.74	0.13	5/5	307	8	176	14	1.66	0.19	4/5	208	5	126	14	
	48.50	B3-48	4-11	25 \pm 5	1.76	0.14	3/3	241	3	137	11	1.67	0.19	4/4	170	8	102	12	
	51.00	B3-51	4-11	25 \pm 5	2.46	0.18	5/5	(212)	3	86	6	2.35	0.25	4/4	(134)	4	57	6	Not considered
	64.00	B3-64	4-11	25 \pm 5	2.30	0.17	5/5	535	10	233**	18	2.20	0.24	7/8	406	5	185**	20	
	85.00	B3-85	4-11	25 \pm 5	2.25	0.16	5/5	628	22	279**	23	2.15	0.23	4/4	412	20	191**	22	
	101.00	B3-101	4-11	25 \pm 5	2.14	0.29	4/4	574	6	268**	36	2.04	0.34	4/4	432	10	212**	35	
B4/12	57.80	Ho-B2-2	4-11	25 \pm 5	1.85	0.16	5/5	550	19	297**	28	1.76	0.22	12/12	375	6	213*	26	

Table 3 continued

Core	Depth (m)	Sample	Fraction (μm)	W_e (%)	Polyminerals fraction (K-Feldspar for coarse-grained samples)			Quartz fraction			Comments								
					D_r (Gy/ka)	\pm	n_{acc}/n_{tot}	D_e (Gy)	\pm	Age (ka)		D_r (Gy/ka)	\pm	Age (ka)					
B5/12	26.00	Ho-B1-9	4-11	25 \pm 5	2.45	0.19	4/5	468	10	191**	16	2.35	0.26	8/8	347	12	147	17	
	29.00	Ho-B1-29	4-11	25 \pm 5	2.57	0.21	4/4	551	9	215**	18	2.46	0.28	5/5	375	10	152	17	
	37.50	Ho-B1-37	4-11	25 \pm 5	2.52	0.18	7/7	522	21	207**	17	2.42	0.25	10/10	370	7	153	16	
	55.95	Ho-B1-8	4-11	25 \pm 5	1.84	0.15	8/8	512	12	278**	23	1.75	0.20	8/8	354	6	202*	24	
	66.50	Ho-B1-7	4-11	25 \pm 5	2.14	0.16	7/7	540	6	253**	19	2.04	0.22	8/8	417	9	204**	23	
	80.00	Ho-B1-6	4-11	25 \pm 5	1.94	0.15	5/5	539	5	277**	21	1.85	0.21	8/8	392	8	212*	24	
	93.22	Ho-B1-5	4-11	25 \pm 5	1.77	0.14	7/7	509	18	288**	25	1.68	0.19	7/7	380	12	226*	27	
	113.35	Ho-B1-3	4-11	25 \pm 5	2.01	0.16	5/5	508	8	253**	20	1.91	0.21	7/8	393	6	206*	23	
	122.80	Ho-B1-2	4-11	25 \pm 5	1.83	0.14	8/8	505	9	276**	22	1.73	0.19	12/12	370	8	214*	25	
	132.80	Ho-B1-1	200-250	20 \pm 5	2.20	0.14	39/40	515	25	234	19	1.36	0.07	12/26	290	22	213*	20	
	145.90	Ho-B1-10	200-250	20 \pm 5	2.17	0.14	16/16	530	40	244	24	1.33	0.07	9/10	205	20	154*	17	
<i>Hardwald, middle Glatt valley</i>																			
KB08-4	52.35	HDB4	4-11	25 \pm 5	2.38	0.17	5/5	597	34	251**	14	2.28	0.24	5/5	396	28	174**	12	
KB08-5	54.50	HDB1	4-11	25 \pm 5	2.50	0.18	5/5	677	22	271**	9	2.39	0.25	5/5	394	57	165**	24	
KB08-7	53.75	HDB2	4-11	25 \pm 5	2.65	0.20	5/5	568	69	214**	26	2.48	0.25	5/5	430	20	173**	8	
	48.72	HDB3	4-11	25 \pm 5	2.30	0.17	5/5	649	29	282**	13	2.20	0.23	5/5	412	21	187**	10	

Bold: reliable ages, type 1, *Age overestimation, type 2, **Saturation limit within error, type 3 (IRSL₅₀ at 470 Gy, quartz OSL at 400 Gy according to Buechi et al. 2017b)

Values in brackets are outliers, not considered, see text. Italic: coarse-grained samples (see text)

W_e estimated paleo-water content, n_{tot} total number of aliquots measured, n_{acc} number of accepted aliquots, n_{sat} number of saturated aliquots, OD overdispersion

unbleached old valley fill, which causes them to overestimate the burial age (see Dehnert et al. 2012; Buechi et al. 2017b). This overestimation can be identified for several samples in Fm D and E, which fall into the age range of 200–240 ka (only Q OSL ages): While the sedimentology of these samples leaves no doubt to their glacially influenced deposition, the apparent burial ages correspond to interglacial MIS7 (Lisiecki and Raymo 2005), which is an ice-free period in the Alpine foreland (Meikirch Interglacial; Preusser et al. 2005, 2011). The ages thus most likely represent overestimated burial ages of deposition during the next younger glacial cycle (MIS6, 130–190 ka; Lisiecki and Raymo 2005), which is an increasingly well dated glacial period in the northern Alpine foreland (Dehnert et al. 2010; Preusser et al. 2011; Bickel et al. 2015; Salcher et al. 2015; Rades et al. 2016). An alternative interpretation is that the apparent MIS7 ages underestimate the true depositional ages, and instead correspond to an older glacial period, e.g. MIS8 or older. Based on the results presented by Buechi et al. (2017b) such a minimum age interpretation of the type 2 burial ages cannot be fully excluded but remains more difficult to explain. For type 2 ages the overlap between Q OSL and IRSL₅₀ ages of some samples cannot be taken as evidence for bleaching of the sample as for type 1 ages as the IRSL₅₀ samples are all in signal saturation (see type 3 below, Dehnert et al. 2012).

Type 3 ages are considered to be minimal ages due to their proximity to the saturation limits determined by Buechi et al. (2017b) for the Glatt valley infill. Many of the IRSL₅₀ ages, many basal Q OSL ages from the LGV cores, and all Hardwald samples fall into this category. Furthermore, most of these ages cannot be considered as reliable minimal age estimates as the lower bounds of these ages may also be affected by incomplete bleaching similar to type 2 ages. Only the Hardwald samples, which have been sampled from lacustrine fines (LFA3.2), can be considered as minimum ages with reliable lower bounds as any age overestimation due to incomplete bleaching would be considered minimal in this sedimentary facies (locally organic-bearing facies, see description in Sect. 4.1). This suggests that the topmost sediments at the Hardwald site are the oldest dated sediments of this study of at least 175 ± 9 ka (cf. Pavoni et al. 2015).

The three coarse-grained samples are in broad agreement with the fine-grained samples. The sedimentology of all these samples from the deeper basin suggests that incomplete bleaching is likely, and thus age overestimation can be expected. The younger age of Ho-B1-10 is likely due to an earlier saturation of the coarse-grained quartz fraction signal (see Buechi et al. 2017b).

Furthermore, three outliers (B1-72, B2-79, B3-51) can be identified with major underestimation relative to the neighbouring samples. This underestimation may be the

result of light exposure during drilling, storage or sampling. Such a scenario is suggested by the poor drill core quality (for B1-72) and the agreement between the two mineral fractions or even younger IRSL₅₀ ages (for B1-72 and B2-79).

Finally, a single piece of heavily deformed and therefore undeterminable wood was found in drill core B5/12 at 44 m depth embedded in LFA5 till (see Fig. 3e). This most likely re-worked wood piece was radiocarbon-dated to an age of > 55.3 ka (beyond ¹⁴C-dating limits; see Supplementary Table 2), which is in broad agreement with the luminescence dating results that indicate a much earlier till emplacement.

5 Discussion

The multiphase erosional and depositional evolution observed in the LGV drill cores can be discussed using nine formations (Fm A–I), which are defined based on lithologic properties, elevation and character of bounding surfaces, as well as chronostratigraphic constraints (Fig. 3). For this purpose, the results of drill cores and outcrops presented above are integrated with existing drill data (Freimoser and Locher 1980; Dr. H. Jäckli AG and DMT GmbH 2012; Dr. von Moos AG 2012). The architecture of these formations is illustrated in five valley cross-profiles (CP-I to CP-V, Fig. 10) and two long profiles (LP-I and LP-II; Fig. 11).

5.1 Erosion and infilling of the deep bedrock troughs (Fm A–E, \geq MIS6)

5.1.1 Formation and evolution of the Strassberg Trough (Fm A–C)

The Quaternary sediments found around the Strassberg Plateau (CP-IV to -V, Fig. 10) can be divided into two fluvial aggradation periods at different base levels (Formations A and C) separated by subglacial trough formation and infilling (Formation B). The oldest stratigraphic element is most likely the fluvial gravels of *Formation A* outcropping over bedrock along the W edge of the Strassberg Plateau with a base elevation of ~ 450 m a.s.l. While the separation of Fm A from Fm C remains uncertain at this site (CP-IV and CP-V, Fig. 10), potential equivalents of Fm A with similar facies and base elevations of ~ 450 – 480 m a.s.l. are found as isolated gravel bodies further up-valley (e.g. CP-I, Figs. 10, 12) and downstream in the Hochrhein valley (e.g. W of Eglisau, Fig. 12; Bitterli-Dreher et al. 2007; Graf 2009). The wide-spread occurrence of these high-lying fluvial gravel suggests that Fm A and its equivalents represent remnants of a gravel

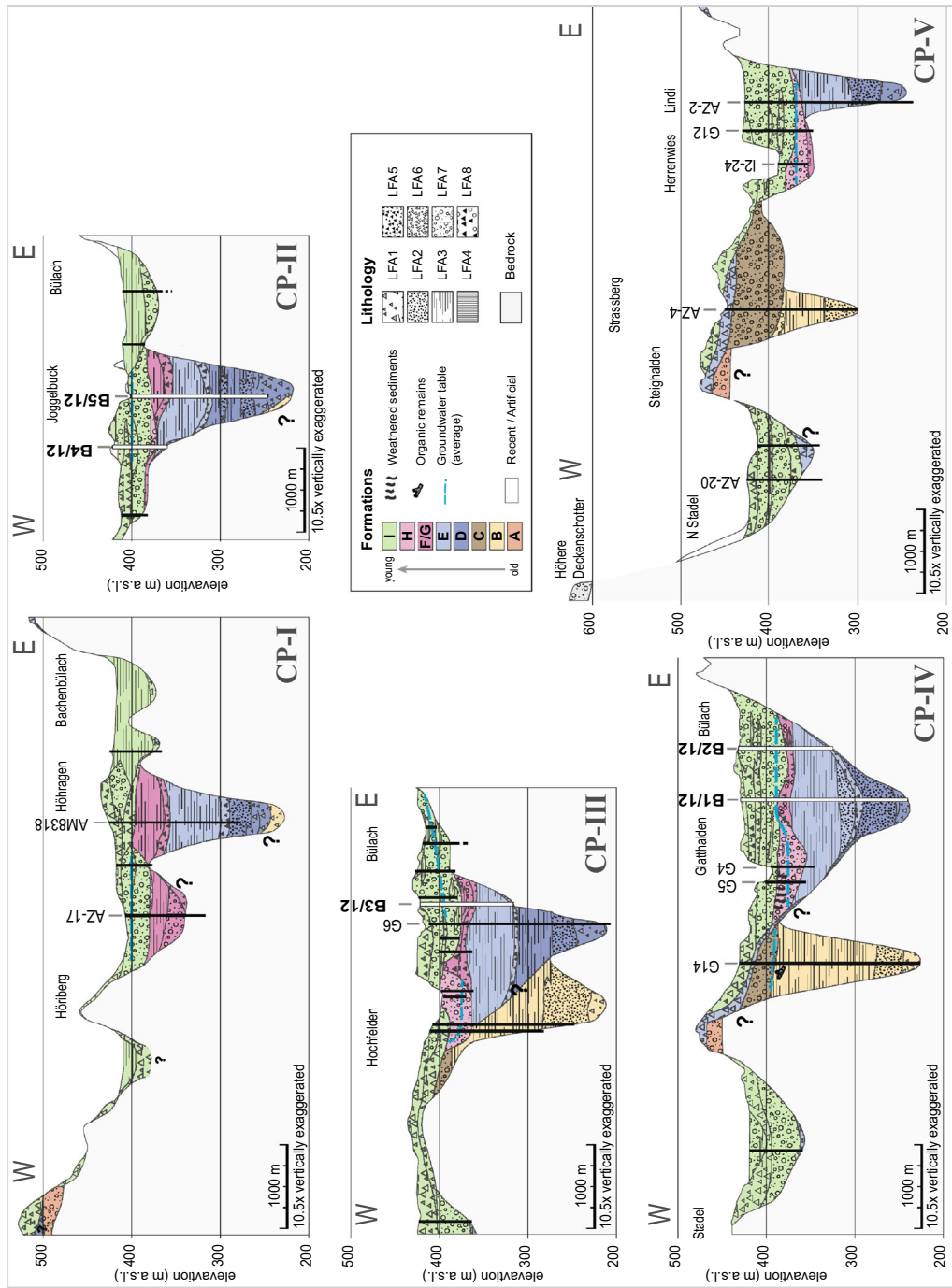


Fig. 10 Schematic profiles across the Lower Glatt valley (CP-I to CP-V). White bars indicate the drillings shown in detail in Fig. 3a-d; black bars are other drillings used for the construction of the profiles (see text). Lithologies are described in Sect. 4.1 and summarized in Table 1. Formations names are indicated with colours and letters A-I (oldest to youngest). Location of the profiles are shown in the Fig. 11 inset

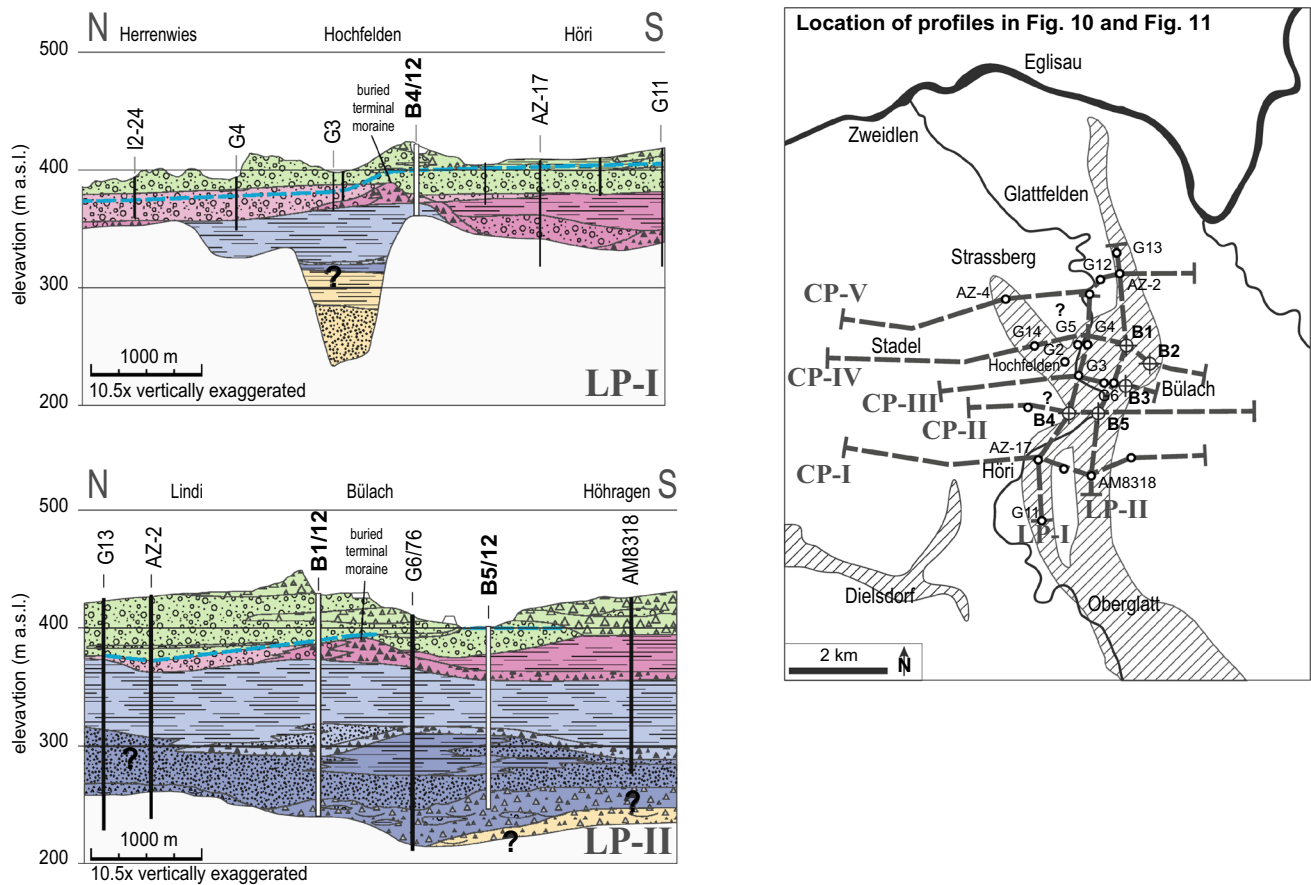


Fig. 11 Schematic longitudinal profiles in the Lower Glatt valley (LP-I and LP-II). White bars indicate drillings shown in detail in Fig. 3a–d; black bars are other drillings used for the construction of

plain that once occupied much of the LGV but underwent strong dissection by later glacial and fluvial erosion (see below, Fig. 12). The aggradation of this Fm A gravel plain can be tentatively attributed to the Habsburg Glaciation (Fig. 13) in agreement with the interpretation of gravel remnants with similar base elevations along the Hochrhein Valley and its tributaries (Fig. 12; Bitterli-Dreher et al. 2007; Graf 2009). A deposition within the context of the poorly constrained Möhlin Glaciation cannot, however, be excluded (Fig. 13).

A first major dissection of Fm A then occurred during the incision of the Strassberg bedrock trough by a glacier that reached at least into the area of the Strassberg Plateau (see Fig. 13). Subglacial erosion of the Strassberg Trough is evidenced by an up to 200 m deep undercutting of the base level constrained by the base elevations of Fm A and C, and an abrupt reverse-sloping termination below the Strassberg Plateau as evidenced by a combination of drill cores and bedrock outcrops (Graf 2009). The sediments infilled into the Strassberg Trough (*Formation B*) are mainly known from flush drill holes G14 and AZ-4 (CP-IV to -V, Fig. 10), which recovered an up to 140 m-thick

the profiles (see text). Lithologies are described in Sect. 4.1 and summarized in Table 1. Formations names are indicated with colours and letters A–I (oldest to youngest)

sequence of LFA2 and 3 sediments representing glacio-deltaic, glacio-lacustrine, and lacustrine deposition (Freimoser and Locher 1980; Dr. H. Jäckli AG and DMT GmbH 2012). Formation B thus documents an infilling of the Strassberg Trough during glacier retreat from the LGV. The onset of deposition, however, may have occurred subglacially as suggested by the coarse-grained deposits at the base of drill hole G14 (Freimoser and Locher 1980), which most likely represent similar tills and subglacial cavity deposits (LFA1) as at the base of the Büelach Trough (Buechi et al. 2017a).

Formation, or at least re-incision, and infilling of the Strassberg Trough is tentatively correlated to the Habsburg Glaciation (Graf 2009; Preusser et al. 2011, see Fig. 13). This glaciation, best documented in the Lower Aare Valley in a similar stratigraphic context, was slightly more extensive than the Birrfeld glaciation (Graf 2009). Translated to the Lower Glatt valley, this position would coincide with the reverse sloping termination of the Strassberg Trough potentially representing the glacier extent at that time (Fig. 2).

Formation C comprises fluvial gravels that overlie the Strassberg Trough and its infill (Fm B). These gravels are

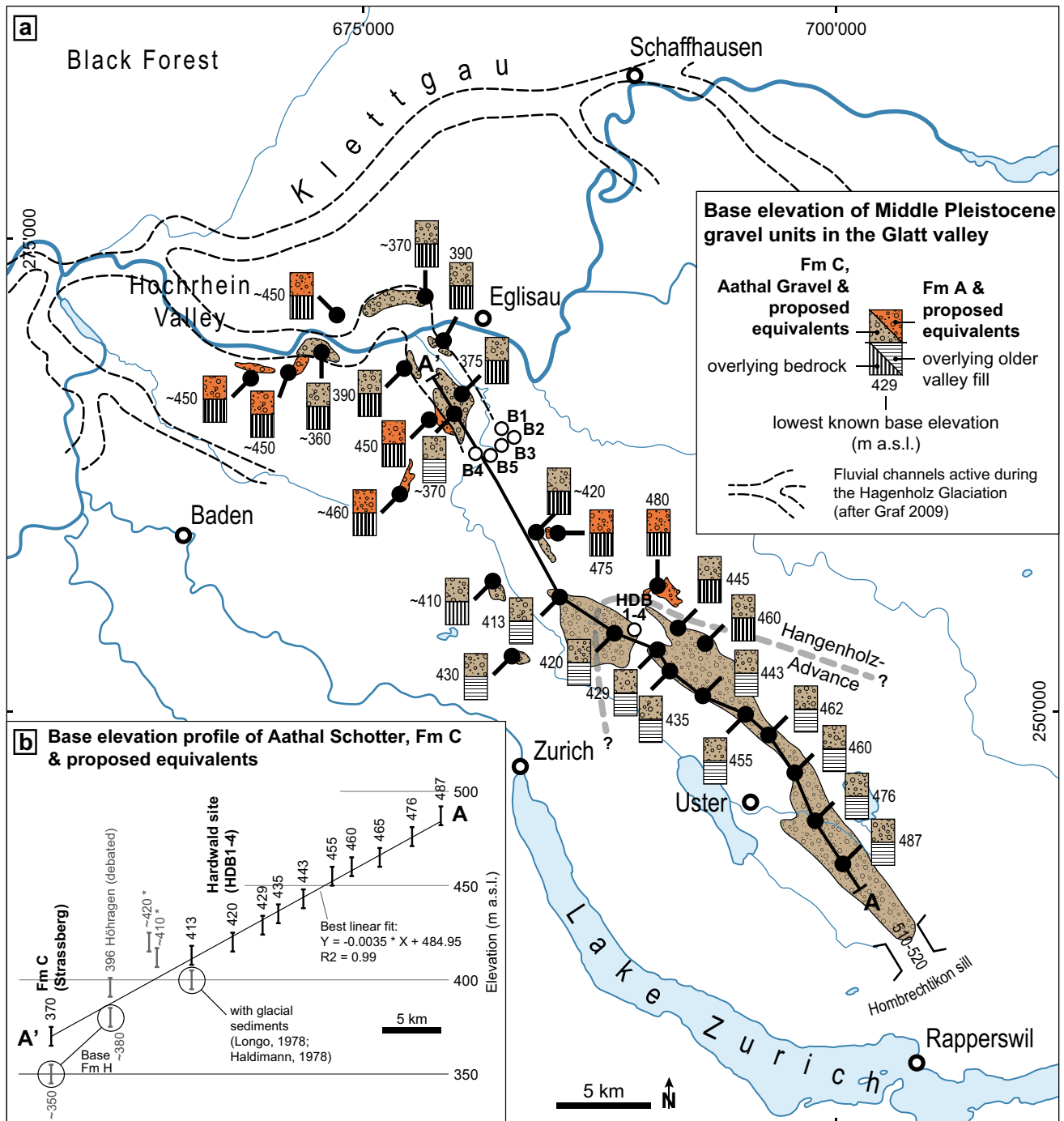


Fig. 12 **a** Map of the distribution and base elevations of Fm A and C gravel remnants and potential equivalents in the Middle and Upper Glatt valley and in the Hochrhein valley. Line A–A’ connects the lowest documented base elevations (black circles) of Fm C which are plotted in inset **b**. **b** Profile A–A’ plots the base elevations of the Aathal Gravel (for locations see **a**) and Fm C along the Glatt valley. Assuming a straight base surface, Fm C in the Lower Glatt valley plots directly on the down-valley extension of this base surface (dashed regression line: projection), whereas base elevation points of Fm H plot below it. This observation may give some support to the

interpretation that Fm C is an equivalent of the Aathal Gravel (see text). A vertical uncertainty of ± 5 m is included. Best linear fit suggests a slope of 0.35% for the base surface. Base elevations of Fm C marked with * have not been considered as no other tie points are available. These points occur over bedrock along the valley sides and are thus likely to lie above the deepest channel base. Subsurface data: Haldimann (1978), Longo (1978), Freimoser and Locher (1980), Kempf et al. (1986), Pavoni et al. (1992), Matousek et al. (2000), Wyssling (2008), Graf (2009) and Rey et al. (2011)

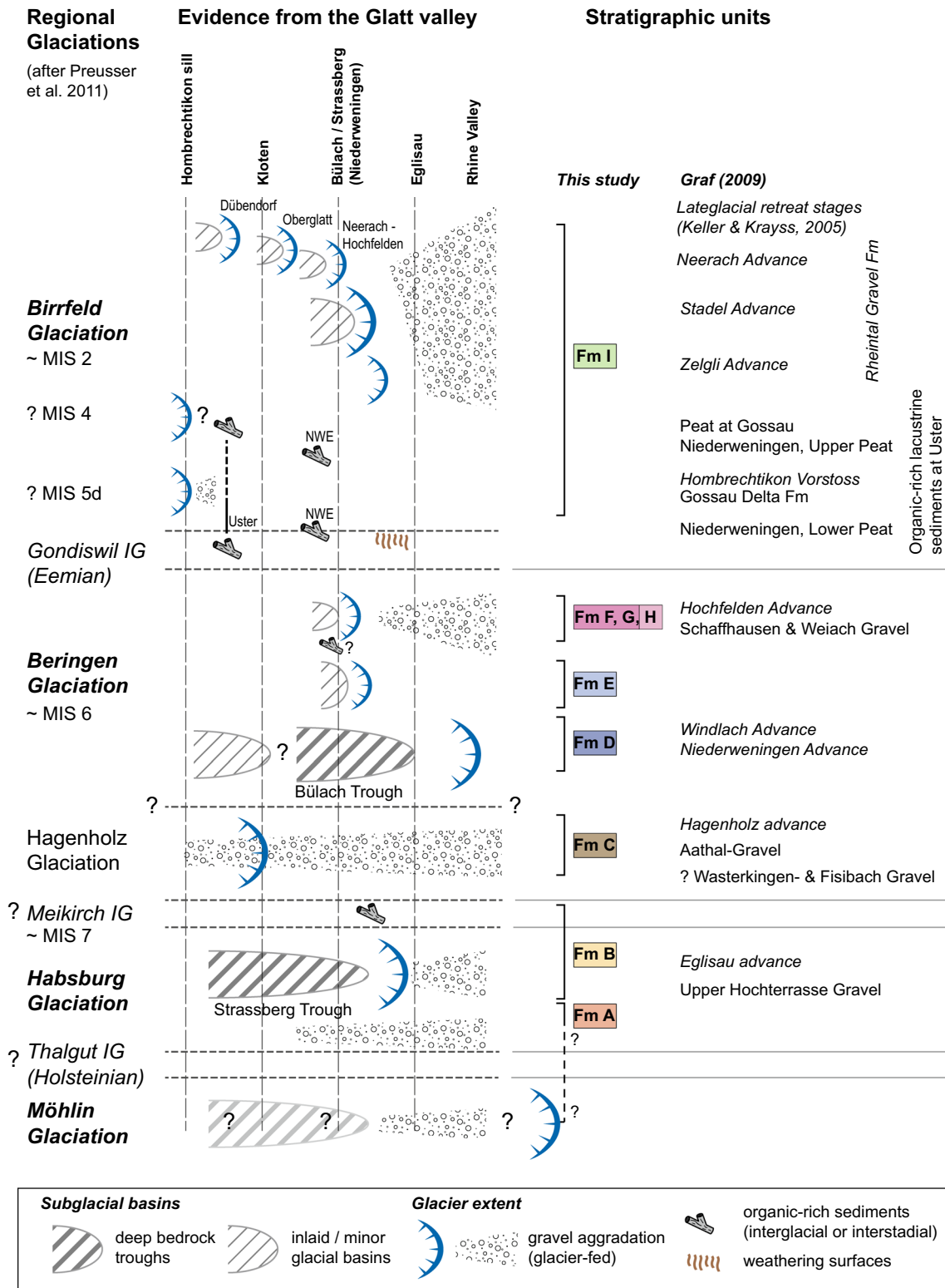


Fig. 13 Summary scheme of the glaciation, basin formation and fluvial aggradation in the Glatt valley during the Middle and Late Pleistocene. IG interglacial, NWE Niederweningen (see text)

of similar facies as Fm A but the base elevations at ~ 370–390 m a.s.l. are distinctly lower and follow a broad fluvial channel incised into Fm B or bedrock (Graf

2009, e.g. CP-V, Fig. 10). Much of the Strassberg Plateau as well as smaller gravel remains towards the Hochrhein valley (Fig. 12a) can be attributed to Fm C, which suggests

that this formation initially formed an extensive gravel plain filling the LGV.

Fm C can be further correlated to gravel plain relicts in the Middle and Upper Glatt valley which are commonly referred to the formation name 'Aathal Gravel' (e.g. Weber 1901; Wyssling 2008). While traditionally attributed to an intermediate terrace level in the LGV based on morphostratigraphy only (e.g. Weber 1928), a correlation with the Fm C on the Strassberg Plateau is supported by the overall very similar facies, composition, and a comparable thickness suggesting glacier-fed aggradation (Hagenholz Glaciation, Fig. 13; Graf 2009; Keller and Krays 2010; Preusser et al. 2011). Furthermore, the channel base of Fm C at ~ 370 m a.s.l. plots on the down-valley extension of the well-constrained base surface of the Aathal Gravel (Fig. 12b). In the LGV, however, care must be exercised before overinterpreting this profile because (1) the base surface is very sensitive to the few points available, and because (2) there are very limited base elevation differences between Fm C and the channel base associated with younger gravels (especially Fm I). In the Upper Glatt valley, Eemian sediments deposited in a basin incised into the Aathal Gravel and the underlying valley fill at Uster (Fig. 12) further suggest that the Aathal Gravel and the underlying valley fill were deposited prior to the last interglacial (Wyssling and Wyssling 1978; Welten 1982), which is in agreement with the interpretation of Fm C as a Middle Pleistocene deposit.

As Fm C can be correlated to the Aathal Gravel, the up to ~ 220 m-thick (glacio-)lacustrine valley fill below the Aathal Gravel could be the equivalent of Fm B, which underlies Fm C in the LGV. At the Hardwald site, the uppermost lacustrine sediments below the Aathal Gravel were interpreted as a minimal age with a reliable lower bound of ~ 180 ka (type 3 age but less affected by incomplete bleaching due to the lacustrine facies). If the correlation based on the similar stratigraphic evolution is correct, then the uppermost fine-grained sediments recovered in the Hardwald and Fm B could also be attributed a similar minimum age. The warmer climatic conditions inferred from wood fragments found in the uppermost part of Fm B and close to the Hardwald site (Longo 1978) could thus represent the MIS7 or an older interglacial.

5.1.2 Formation and evolution of the Bülach Trough and the lower inlaid glacial basin (Fm D–E)

After deposition of Fm C, the Glatt valley glacier advanced again into the LGV where it overrode the Fm C gravel plain (indicated by overlying glacial sediments (Fig. 2a) and broken clasts (Fig. 7c)), dissected it, and incised the Bülach Trough, which can be traced as far as Eglisau where it ends abruptly with a reverse slope

(Fig. 2b). This scenario of a cutting stratigraphic relationship between Fm C and the Bülach Trough suggests a relatively younger age for the Bülach Trough than the Strassberg Trough, which is overlain by gravels of Fm C. This relationship is supported by the following arguments: Firstly, the gravels of Fm C are absent above the Bülach Trough, while isolated remnants along the valley (Fig. 12) are clear evidence for an initially much more wide-spread occurrence of Fm C in the form of a gravelly valley fill. Before incising the Bülach bedrock trough, Fm C must thus have been eroded. Secondly, Fm C overlying the Strassberg Trough is very different to the stratigraphic succession that overlies the Bülach Trough. The latter succession comprises fluvial channels (see Fm H) with a ~ 20 – 30 m lower base elevation than Fm C. Thirdly, hydrogeological investigations suggest that the aquifer in Fm C gravels is disconnected from the aquifer in the gravelly deposits on top of the Bülach Trough. This evidence was taken as an indication for a low permeable boundary, potentially a till, separating these two aquifers (Freimoser and Locher 1980).

The onset of deposition in the Bülach Trough comprises emplacement of subglacial tills and meltwater deposits (LFA1 in B1-, B5/12 and G6) followed by a thick glacier-retreat sequence with sub-marginal or proximal glacio-deltaic (LFA2) to glacio-lacustrine (LFA3) sedimentation (*Formation D*). The vertical succession of sands and fines (LFA2, 3) is interpreted as a back-stepping of deltaic sedimentation in favour of fine-grained glacio-lacustrine sedimentation during glacier retreat.

This sequence is truncated by a subglacial till (LFA5) documented in drill cores that recovered the deeper infill of the Bülach Trough (B1-, B5/12, G6, and potentially also AM8318, see LP-II, Fig. 11). This till is interpreted as a glacier re-advance into the Bülach Trough at least as far as drill hole B1/12. It eroded parts of the underlying infill as suggested by the truncated lower retreat sequence and the dark, matrix-supported character of the LFA5 till is interpreted to result from reworking of glacio-lacustrine sediments. The vertical position of the intermediate till coincides with a widening of the cross-section of the bedrock trough. This broader cross-section can be traced to a similar spatial extent as this intermediate till, which together suggest a second glacial basin generation forming an inlaid basin in the Bülach Trough. This inlaid basin is also in an overdeepened position, but apparently did not incise the trough base deeper into bedrock, but rather widened the pre-existing basin. The inlaid basin was subsequently filled by glacio-deltaic and glacio-lacustrine sediments (*Formation E*) interpreted as a second glacier retreat sequence similar to *Formation D*.

Final deposition in the Bülach Trough (Fm E) occurred ~ 130 – 150 ka, i.e. at the end of MIS6 as reliably constrained by type 1 ages from the uppermost lacustrine

sediments of Fm E in cores B1-, and B2/12. With depth, the dating results are increasingly influenced by inherited burial doses (type 2 ages) for which an MIS6 age is inferred (Buechi et al. 2017b). While the possibility of an older than MIS6 age for these samples lower down in the drill core cannot be completely ruled out (Buechi et al. 2017b), the consistent glacier retreat sequence leaves little room for a major undetected unconformity separating the upper reliable MIS6 ages from an older valley fill further down. The limited growth of the burial doses across the unconformity marked by the till at the base of Fm E is unlikely to represent a major time gap. Instead, the very similar burial doses for Fm D and E may support the sedimentological interpretation of this till as a result of a glacier re-advance into the Bülach Trough during the same glaciation rather than during a separate glacial cycle.

5.1.3 Formation of the upper inlaid basin and establishment of the lowest fluvial channel (Fm F–H, 130–150 ka)

The subglacial to lacustrine Bülach Trough infill (Formations D–E) is unconformably overlain by glacial sediments summarized as Formation F. At the base of Fm F, a subglacial till (LFA5) is found in drill cores as far north as B3/12 indicating a glacier advance into the area of Bülach. In this terminal position, the glacier appears to have formed a terminal moraine (today buried below younger gravelly sediments of Fm I). The position of this terminal moraine ridge is, however, indicated by the lateral and vertical succession of tills (mostly LFA5), ice-proximal gravels and diamicts (LFA8) and LFA7 gravels (for location see LP-I and LP-II, Fig. 11). Furthermore, this interpretation is supported by earlier observations by Freimoser and Locher (1980) who related the marked drop of the groundwater table at this position to a buried terminal moraine acting as a groundwater barrier (Figs. 10, 11).

On the inner-side of the terminal moraine deposits, a LFA5 till unit occurs down to ~ 360 m a.s.l., which suggests that during this glaciation a second inlaid glacial basin was carved into the existing valley fill (LP-II, Fig. 11). This partial erosion of the fine-grained valley fill (Fm E) is documented by the wide occurrence of the dark, matrix-rich till facies (see LFA5 description) and may explain a small piece of deformed wood found at the base of this formation. The erosion of the minor Höri basin (Fig. 2b) is tentatively associated with the same period (around AZ-17, CP-I and LP-I).

Within the extent of this newly formed basin, the LFA5 tills are directly overlain by lacustrine sediments (LFA3), which indicate that a lake occupied this upper inlaid basin after deglaciation (Formation G). The overall thickness of the lacustrine sequence in Fm G is ~ 35 m, with the

highest lacustrine sediments occurring at ~ 395 m a.s.l. (see Line I, Fig. 10, excluding the glacio-deltaic deposits in the deepest part of AZ-17). Such a relatively high level indicates that the lake in which they were deposited was dammed by an intact terminal moraine at Bülach (Fm F). The reconstructed crest elevation of this moraine (see LP-I and LP-II, Fig. 11) is in broad agreement with this interpretation, but the preserved morphology is likely to have been degraded by subsequent fluvial and glacial action.

The burial ages of Fm G are ~ 130 – 150 ka and thus the same, within errors, as the youngest ages of the underlying thick valley fill (Fm E). The timing of till deposition and glacier advance into the Bülach area (Fm F) is therefore bracketed to a late MIS6 period and is considered to be a late re-advance of the Beringen Glaciation. Additional samples taken from thin lacustrine units in LFA8 agree with this interpretation.

On the outer side of this buried terminal moraine at Bülach, the ~ 30 m thick fluvial gravel of Formation H was deposited into a newly incised channel (base of Fm H in LP-I, Fig. 11). The base of this channel is the deepest known from the Bülach area with a base sloping from ~ 360 to 350 m a.s.l. between profiles CP-II and CP-V (Fig. 10). Fluvial incision and aggradation are interpreted to have occurred in direct response to the glacier advance and stagnation at the Bülach terminal moraine. Shallow lake formation and weathering of the top surface of Fm H (see drill core G5 in CP-IV Fig. 10 and drill core B4/12) may indicate exposure and conditions favourable for weathering and soil formation and can tentatively be associated with the last interglacial period.

A continuation of the deepest fluvial channel infilled with Fm H exists between Bülach and Zweidlen (Fig. 14). Together with the equivalent fluvial bedrock channel between Schaffhausen and Zurzach, this drainage system forms the lowest Pleistocene base level in north-eastern Switzerland (Hug 1907; Graf 2009; Fig. 14). This correlation is supported by a depositional age of ~ 130 – 159 ka for the channel fill south of Schaffhausen (Schaffhausen Gravel, Preusser and Graf 2002; Lowick et al. 2015). The U/Th age of 40 ± 5 ka for the cementation of the correlated Weiach Gravel (Graf 2009) is also in agreement with this interpretation. Furthermore, the stratigraphic succession at the Weiach site with a distinct weathered top surface overlain by last glacial fluvio-glacial sediments is similar to that of Fm H.

The incision of this channel is most likely attributed to the southward deflection of the Rhine River at the end of the Beringen glaciation, which occurred due to the blockage of the former river course through the Klettgau by glacial deposits (e.g. Graf 2009; Fig. 14). Between Zweidlen and Zurzach the newly incised Rhine River followed pre-existing fluvial channels of the Glatt and Töss Rivers.

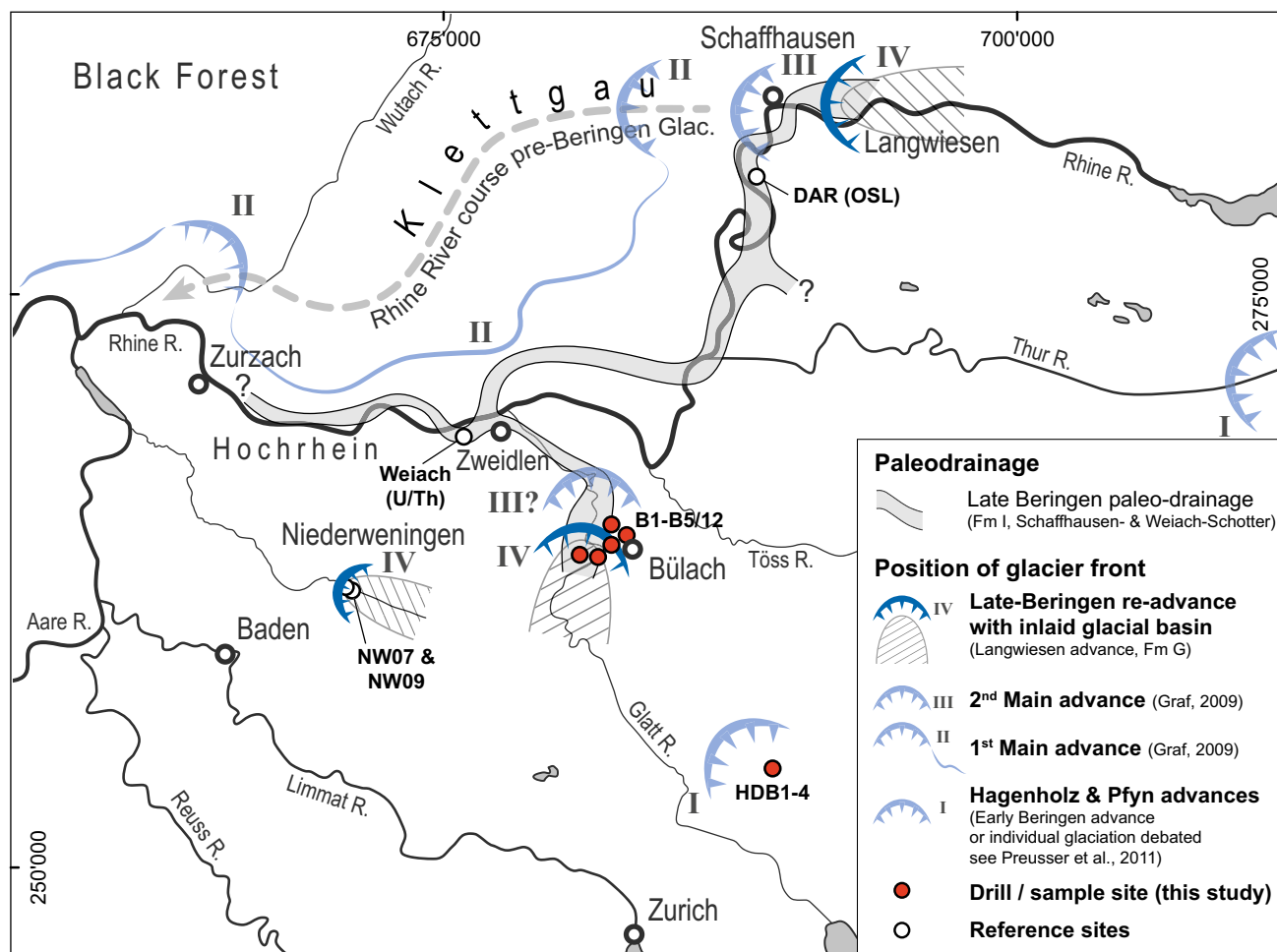


Fig. 14 Schematic illustration of the inferred ice-margin position during the Beringen Glaciation (\sim MIS6) with emphasis on evidence for a Late Beringen re-advance (frontal position IV) in the Glatt valley and surrounding areas at the end of MIS6 (\sim 150–130 ka). Together with the most extensive Beringen Glaciation advances (frontal positions II and III) and a potential early advance into the Middle Glatt valley (frontal positions I, Hagenholz advance) a total of

up to four glaciation phases can be distinguished. DAR: Dachsen OSL sampling site of the Schaffhausen Gravel Fm (Preusser and Graf 2002; Graf 2009; Lowick et al. 2015); Weiach (U/Th): U/Th sampling site of the Weiach Gravel Fm (see Graf 2009); NW07: Anselmetti et al. (2010); NW09: Dehnert et al. (2012). Paleo-channel and Beringen maximum extent modified after Graf (2009)

However, the coupling of the Rhine catchment into these 2–3 orders of magnitude smaller river systems caused a massive increase in discharge and thus sediment transport and erosional efficiency (Knighton 1998). The river profile is likely to adjust to such step changes by incision as modelled for similar river captures in the northern Alpine foreland (e.g. Yanites et al. 2013). Such a scenario may explain the incision to such a low channel base.

An equivalent to the late-Beringen Glaciation re-advance in the Bülach area is potentially documented in drill cores to the east of Schaffhausen, where subglacial tills forming a minor inlaid basin are associated with the Schaffhausen Schotter (Langwiesen Advance, Graf 2009; Fig. 14). Evidence for such a glacier re-advance also comes from the Wehntal, where lacustrine sediment deformation, consolidation and erosion observed in drill

cores were interpreted as a glacier re-advance that could be constrained to a very similar age (Anselmetti et al. 2010; Dehnert et al. 2012).

During glacier retreat and lake formation behind the terminal moraine, the Glatt River appears to have eroded back into the terminal moraine ridge around Hochfelden. The location of this breach is poorly documented, but may coincide with the location of a preferred groundwater flow corridor in this area indicating a connection of the groundwater bodies on either side of the terminal moraine (see Dr. von Moos AG 2012). The lowering of the moraine dam consequently caused the lake level to drop, and the Glatt River to incise into the lake sediments of Fm G to some extent. This is supported by the uneven top surface of Fm G documenting erosion and weathered sediments in B4/12 at around 380 m a.s.l. (internal slope of the terminal

moraine, LFA8). These gravels and diamicts could represent instability of the internal moraine slope during incision followed by later exposure and soil formation. The erosional and partly weathered top surface of LFA8 sediments defines the top of Fm H within the terminal moraine.

The upstream continuation of the fluvial gravel of Fm H is indicated in the profiles (e.g. gravels overlying Fm G in LP-I between B4/12 and AZ-17, Fig. 11), but remains poorly constrained due to a later fluvial and glacial overprint. The base-level drop along the Hochrhein is likely to have propagated upstream and may later also have reached the Niederrhein area, where it may have caused the switch from lacustrine to peat deposition documented around 120–130 ka (Anselmetti et al. 2010; Dehnert et al. 2012).

5.1.4 Fluvial aggradation and last glaciation (Fm I, < MIS6)

The base of Formation I contains well-sorted fluvial gravels (LFA7.1) infilled into broad fluvial channels (CP-II to -V, Fig. 10). Thin lacustrine interbeds occurring at the base of Fm I can be constrained to ~ 80–40 ka, which corresponds to the early last glacial cycle (late MIS5-3). This depositional phase is followed by a glacier advance sequence consisting of thick-bedded coarsening-upward fluvial to fluvio-glacial gravels with boulder layers (typically LFA7.1 followed by LFA7.2 in B1/12-B3/12, see Fig. 3) and topped by interbedded tills and gravels (LFA6, 7, 8). This sequence can be correlated to the build-up of ice in the Alpine foreland after ~ 30 ka and the tills broadly represent the period of maximum extent of the Late Birmfeld Glaciation, synchronous with the global last glacial maximum (~ 24–22 ka; Ivy-Ochs et al. 2004, 2008; Preusser 2004; Keller and Krayss 2005; Preusser et al. 2011).

A first advance may have reached as far as Glattfelden as suggested by diamictons documented in several drill cores north of Bülach (AZ-2, G12, G13, etc., see Graf 2009). In cores B1- and B2/12, the tills of this first advance in Fm I are overlain by a succession of at least another two LFA6 till beds separated by fluvio-glacial and ice-marginal deposits (LFA7.2 and LFA8). This vertical facies succession most likely represents an oscillation of the glacier front in the area of Bülach, which is also documented in the Stadel area (CP-IV to -V, Fig. 10; Freimoser and Locher 1980; Graf 2009). The uppermost tills are connected to the Stadel-Bülach terminal moraine (see Fig. 2a and CP-III to -V, Fig. 10). To the north, these tills interfinger with gravels (LFA8, 7) interpreted as glaciofluvial and fluvial outwash deposits that build the extensive gravel plains towards the Hochrhein valley (Freimoser and Locher 1980). Similar stacked till-gravel sequences are also recovered in the Hochfelden area (e.g. B4/12 and AM8318, CP-I and CP-II, Fig. 10), where they are related to the terminal moraines of the Neerach-Hochfelden retreat stage (Fig. 2a). With

further glacier retreat, the Glatt River incised up to ~ 40 m into Formation I including a narrow canyon-like breach through these terminal moraines.

6 Stratigraphy of subglacial basin and patterns of subglacial erosion

The evidence presented here suggests that incision of the Bülach Trough and subsequent infilling most likely occurred during the Beringer Glaciation. The continuous facies evolution indicates that also the emplacement of tills and subglacial cavity deposits at the base of the trough (LFA1) falls into this glaciation. The markedly lower carbonate contents in these subglacial sediments further suggest that eroded local bedrock with a low carbonate content is a major constituent (see Sect. 4.3). The fingerprint of the local bedrock lithology is only likely to be preserved if bedrock incision has occurred shortly before emplacement of the subglacial sediments, or alternatively at the same time, but spatially apart (see Buechi et al. 2017a). Such a prompt incision and infilling scenario may, by analogy, also apply for the Strassberg Trough and its infill, although during an earlier Middle Pleistocene glaciation, probably the Habsburg Glaciation (Fig. 13). While a trough re-excavation and/or deepening along pre-existing basins cannot be excluded per se, the narrow shape of both troughs in the LGV (e.g. CP-IV and CP-V, Fig. 10) is difficult to explain as the result of several glaciations. Analogous to the formation of the lower inlaid basin in the Bülach Trough, we would rather expect that repeated occupation of the bedrock trough in combination with the relatively weak bedrock lithologies causes a widening of the cross-sectional geometry. The reason for the formation of two sub-parallel bedrock troughs remains, however, unclear. Such parallel or bi-furcating bedrock troughs in ice-marginal areas suggest, however, that the re-excavation of existing troughs is not a priori favoured.

South of Bülach in the area of the Höhragen and Kloten Troughs (Fig. 2b), the Bülach and Strassberg Troughs can no longer be distinguished in terms of the bedrock morphology and re-activation of existing bedrock troughs is the most likely scenario (CP-I to -III, Fig. 10). For this area, it is interpreted that the glaciation, which was responsible for the Bülach Trough formation, incised into existing basin fill that represents the up-valley extension of the Strassberg Trough. This up-valley correlation of the bedrock trough and the existence of a bifurcation remain, however, poorly constrained and additional subsurface data, e.g. drill holes and geophysical data, are needed to assess the bedrock geometry and the potential intersection of the two basin fills.

Apart from these bedrock troughs, second-order 'inlaid' basin generations are important to reconstruct glacier

dynamics. In the Bülach Trough, such inlaid basins appear to have formed by two re-advances during the Beringen Glaciation. While the basin unconformity of these inlaid basins is a LFA5 till in both cases, the first re-advance caused a widening of the existing bedrock trough, as it potentially advanced into an underfilled basin, whereas the second re-advance is documented only by minor basin formation, which may indicate the limitations of such re-advances to carve basins into fine-grained, glacio-lacustrine substrates with low permeability (e.g. Menzies 1989). The pattern of these Beringen-aged glacial basins furthermore appears to be similarly documented for the penultimate glacial cycle of the neighbouring Lake Constance area (Graf 2009; Ellwanger et al. 2011).

Two, partially separated, valley fills are then again documented in the Upper Glatt valley, where a potential Beringen-aged basin, equivalent to the Bülach Trough, appears to be inlaid into an older, broad bedrock trough equivalent to the Hardwald site and the Strassberg Trough, respectively (Wyssling and Wyssling 1978; Wyssling 2008; Graf 2009). This could indicate that the subglacial erosion of the Beringen glaciation was less in the Upper Glatt valley, creating an inlaid glacial basin and preserving more the older valley fill including much of the Aathal Gravel. In contrast, subglacial erosion was more intense further downstream in the LGV, where less of the Aathal Gravel equivalent (Fm C) was preserved.

The arrangement of these subglacial basins in the Glatt valley with different sub-parallel or bifurcating bedrock troughs, re-excavated segments, and inlaid basins document changes in the magnitude and spatial focus of subglacial erosion over time. These changes are poorly understood but may reflect a combination of the paleoglaciological conditions (glacier extent, basal temperatures, meltwater fluxes, e.g. Piotrowski 1994; Hooke and Jennings 2006), glacier bed permeability and topography (e.g. Menzies 1989), and feedbacks promoting or limiting subglacial erosion (e.g. glacio-hydraulic super-cooling; Fountain and Walder 1998; Cook and Swift 2012). While some of these factors reflect primarily local conditions, the overall basin stratigraphy is likely to be dominated by a climatic control on glacier growth and decay.

7 Summary and conclusions

The reconstruction of the Quaternary landscape evolution of the Lower Glatt valley (LGV) illustrates the large impact that repeated glaciation exerts on an orogen and its foreland. Bedrock surface and valley fills are the result of multiple erosion and infilling cycles, and reflect the interplay of subglacial erosion, glacial to lacustrine infilling of overdeepened basins, and fluvial down-cutting and

aggradation in the non-overdeepened valley fill. Reworking of existing valley fill material is omnipresent. Our detailed geomorphologic, sedimentologic, and chronostratigraphic analysis thus reveals a succession of erosion and depositional cycles that can serve as a model for other glaciated mountain ranges similar to the Alps and their foreland during the Middle and Late Pleistocene.

The three to four major glaciation phases that can be reconstructed in the LGV (Fig. 13) correspond to (1) the maximum extent of the Birrfeld Glaciation with minor basin formation, ice-front oscillation and fluvio-glacial aggradation and several retreat stages (\sim MIS2); (2) the Beringen Glaciation with most likely three basin sequences, i.e. the Bülach bedrock trough and two inlaid basins (\sim MIS6); (3) the Hagenholz Glaciation, documented with major gravel accumulation in the LGV and ice-contact in the Middle Glatt valley. This glaciation could alternatively represent an early Beringen Glaciation advance; and iv) the least constrained Habsburg/Möhlin Glaciations probably responsible for the oldest basin generation in the LGV so far constrained by the Strassberg Trough and its infilling before \sim 180 ka as inferred from the Hardwald site. The uncertainties associated with the luminescence dating of the Bülach valley fill (type 2–3 ages) encourage future testing with other luminescence signals and other dating methods. Interglacial periods are highly underrepresented and the importance of organic remains identified at older drill sites may also direct future research.

The separate Strassberg- and Bülach Troughs confirm that localized subglacial erosion was active during different Middle Pleistocene glaciations. However, caution is advised before relying on the bedrock unconformities alone, as these may be highly time-transgressive. Instead, this study promotes a closer consideration of the infilled basin sequences and inlaid basins. For the MIS6 Beringen Glaciation, for instance, a three- to four-stage evolution in agreement with regional stratigraphy is proposed (Fig. 14). Systematic valley fill analysis may thus elucidate changes in focus and magnitude of subglacial erosion over time and the reconstruction of glacial basin generations may therefore provide a powerful tool for the reconstruction of extent, timing, and characteristics of past glaciations.

Acknowledgements The authors would like to thank W. Blüm and the environmental agency of the Canton of Zurich (Office of Waste, Water, Energy and Air, AWEL) for leaving the drill cores at our disposal. The National Cooperative for the Disposal of Radioactive Waste (Nagra) provided logistic support with the drill-core boxes, contributed the regional bedrock surface model and co-funded S. Lowick. M. Pfiffner and P. Hayoz, Swiss Geologic Survey, provided storage and work space at the Swisstopo core repository. F. Preusser and G. Deplazes are thanked for sampling the Hardwald drill cores and discussion. Gamma spectrometric measurements were performed by S. Szidat, Department of Chemistry and Biochemistry, University of Bern. Technical support was provided by J. Krbanjevic (bulk

geochemistry measurements, University of Bern), J. Oberžan, and B. Bellwald (both for core preparation). SEAG and W. Leu are thanked for providing the documentation of drill hole AM8318. R. Zech is acknowledged for finding and radiocarbon dating the wood pieces. The manuscript further benefited from discussions with S. Frank and J. Menzies. We thank associate-editor Christian Schlüchter, Erich R. Müller, and an anonymous reviewer for their helpful suggestions.

References

- Anselmetti, F. S., Drescher-Schneider, R., Furrer, H., Graf, H. R., Lowick, S., Preusser, F., et al. (2010). A ~180,000 years sedimentation history of a perialpine overdeepened glacial trough (Wehntal, N-Switzerland). *Swiss Journal of Geosciences*, *103*, 345–361.
- Beck, P. (1933). Über das schweizerische und europäische Pliozän und Pleistozän. *Eclogae Geologicae Helveticae*, *26*, 335–437.
- Benn, D. I., & Ballantyne, C. K. (1993). The description and representation of particle shape. *Earth Surface Processes and Landforms*, *18*, 665–672.
- Benn, D. I., & Ballantyne, C. K. (1994). Reconstructing the transport history of glacial sediments: a new approach based on the covariance of clast form indices. *Sedimentary Geology*, *91*, 215–227.
- Bickel, L., Lüthgens, C., Lomax, J., & Fiebig, M. (2015). The timing of the penultimate glaciation in the northern Alpine Foreland: New insights from luminescence dating. *Proceedings of the Geologists' Association*, *126*, 536–550.
- Bini, A., Buoncristiani, J. F., Couterrand, S., Ellwanger, D., Felber, M., Florineth, D., et al. (2009). *Die Schweiz während des letzteiszeitlichen Maximums (LGM), 1:500'000*. Wabern: Bundesamt für Landestopographie.
- Bitterli-Dreher, P., Graf, H. R., Naef, H., Diebold, P., Matousek, F., Burger, H., et al. (2007). *Geologischer Atlas der Schweiz. 1070 Uster (Atlasblatt 120). Erläuterungen*. Wabern: Bundesamt für Landestopografie.
- Bodenburg Hellmund, H. W. (1909). Die Drumlinlandschaft zwischen Pfäffiker- und Greifensee (Kanton Zürich). *Vierteljahrsschrift der Naturforschenden Gesellschaft in Zürich*, *54*, 149–216.
- Boulton, G. S., & Paul, M. A. (1976). The influence of genetic processes on some geotechnical properties of glacial tills. *Quarterly Journal of Engineering Geology and Hydrogeology*, *9*, 159–194.
- Buechi, M. W., Frank, S. M., Graf, H. R., Menzies, J., & Anselmetti, F. (2017a). Subglacial emplacement of tills and meltwater deposits at the base of overdeepened bedrock troughs. *Sedimentology*, *64*, 658–685. <https://doi.org/10.1111/sed.12319>.
- Buechi, M. W., Lowick, S. E., & Anselmetti, F. S. (2017b). Luminescence dating of glaciolacustrine silt in overdeepened basin fills beyond the last interglacial. *Quaternary Geochronology*, *37*, 55–67. <https://doi.org/10.1016/j.quageo.2016.09.009>.
- Carr, S. (2004). Micro-scale features and structures. In D. J. A. Evans & D. I. Benn (Eds.), *A practical guide to the study of glacial sediments* (pp. 115–144). London: Hodder Education.
- Charrad, M., Ghazzali, N., Boiteau, V., & Niknafs, A. (2014). NbClust: An R package for determining the relevant number of clusters in a data set. *Journal of Statistical Software*, *61*, 1–36.
- Cook, S. J., & Swift, D. A. (2012). Subglacial basins: Their origin and importance in glacial systems and landscapes. *Earth-Science Reviews*, *115*, 332–372.
- Dehnert, A., Lowick, S. E., Preusser, F., Anselmetti, F. S., Drescher-Schneider, R., Graf, H. R., et al. (2012). Evolution of an overdeepened trough in the northern Alpine Foreland at Niederweningen, Switzerland. *Quaternary Science Reviews*, *34*, 127–145.
- Dehnert, A., Preusser, F., Kramers, J. D., Akçar, N., Kubik, P. W., Reber, R., et al. (2010). A multi-dating approach applied to proglacial sediments attributed to the Most Extensive Glaciation of the Swiss Alps. *Boreas*, *39*, 620–632.
- Dreimanis, A. (1979). The problems of waterlain tills. In: Schlüchter C. (Ed.), *Moraines and varves. Origin, genesis, classification* (pp. 167–177). Proceedings of an INQUA Symposium on Genesis and Lithology of Quaternary Deposits. Rotterdam: A.A. Balkema.
- Dr. H. Jäckli AG (2008). *Technische Untersuchung, Deponie Hardwald, Dietlikon und Bassersdorf/ZH*. Technical report, unpublished.
- Dr. H. Jäckli AG, & DMT GmbH-Co. KG (2012). 2D-Seismik Nordschweiz 2011/12: Geologische Aufnahme der Aufzeitbohrungen (Teil 1) und Aufzeitmessungen (Teil 2). *Nagra Arbeitsbericht NAB 12-22*. Wettingen: Nagra.
- Dr. von Moos AG (2012). *Grundwasserstudie Bülach-Hochfelden. Auswertung der Bohrkampagne 2011/2012*. Technical report, Nr. 9666_9667 on behalf of AWEL, Abt. Gewässerschutz, Kanton Zürich.
- du Pasquier, L. (1891). Die fluvioglacialen Ablagerungen der Nordschweiz. *Beiträge zur geologischen Karte der Schweiz, Neue Folge, 1. Lieferung*. Geologische Kommission der Schweizerischen Naturforschenden Gesellschaft.
- Dürst Stucki, M., & Schlunegger, F. (2013). Identification of erosional mechanisms during past glaciations based on a bedrock surface model of the central European Alps. *Earth and Planetary Science Letters*, *384*, 57–70.
- Ellwanger, D., Wielandt-Schuster, U., Franz, M., & Simon, T. (2011). The Quaternary of the southwest German Alpine Foreland (Bodensee-Oberschwaben, Baden-Württemberg, Southwest Germany). *Quaternary Science Journal*, *60*, 306–328.
- Evans, D. J. A., & Benn, D. I. (2004). Facies description and the logging of sedimentary exposures. In D. J. A. Evans & D. I. Benn (Eds.), *A practical guide to the study of glacial sediments* (pp. 11–51). London: Hodder Education.
- Eyles, N., Eyles, C. H., & Miall, A. D. (1983). Lithofacies types and vertical profile models; An alternative approach to the description and environmental interpretation of glacial diamict and diamictite sequences. *Sedimentology*, *30*, 393–410.
- Fiebig, M., Herbst, P., Drescher-Schneider, R., Lüthgens, C., Lomax, J., & Doppler, G. (2014). Some remarks about a new Last Glacial record from the western Salzach foreland glacier basin (Southern Germany). *Quaternary International*, *328–329*, 107–119.
- Fountain, A. G., & Walder, J. S. (1998). Water flow through temperate glaciers. *Reviews of Geophysics*, *36*, 299–328.
- Freimoser, M., & Locher, T. (1980). Gedanken zur pleistozänen Landschaftsgeschichte im nördlichen Teil des Kantons Zürich aufgrund hydrogeologischer Untersuchungen. *Eclogae Geologicae Helveticae*, *73*, 251–270.
- Graf, H. R. (1993). Die Deckenschotter der zentralen Nordschweiz. *Ph. D. dissertation*, ETH Zürich.
- Graf, H. R. (2009). Stratigraphie von Mittel- und Spätpleistozän in der Nordschweiz. *Beiträge zur Geologischen Karte der Schweiz (N.F.)*, *168*. Wabern: Landesgeologie, Swisstopo.
- Graf, H. R., & Hofmann, F. (2000). Zur Eiszeitgeologie des oberen Klettgau. *Jahresberichte und Mitteilungen des Oberrheinischen Geologischen Vereins*, *82*, 279–315.
- Green, A. G., Merz, K., Marti, U., & Spillmann, T. (2013). Gravity data in northern Switzerland and southern Germany. *Nagra Arbeitsbericht NAB 13-40*. Wettingen: Nagra.

- Haldimann, P. (1978). Quartärgeologische Entwicklung des mittleren Glattals (Kt. Zürich). *Eclogae Geologicae Helveticae*, 71, 347–355.
- Hantke, R. (1959). Zur Altersfrage der Mittelterrassenschotter. *Vierteljahrsschrift der Naturforschenden Gesellschaft in Zürich*, 104, 1–47.
- Hantke, R. (1967). Geologische Karte des Kantons Zürich und seiner Nachbargebiete. *Vierteljahrsschrift der Naturforschenden Gesellschaft in Zürich*, 112, 91–122.
- Hantke, R. (1978). Eiszeitalter. *Die jüngste Erdgeschichte der Alpen und ihrer Nachbargebiete. Teil 1: Klima, Flora, Fauna, Mensch; Alt- und Mittelpleistozän; Vogesen, Schwarzwald, Schwäbische Alb, Adelegg*. Thun: Ott Verlag.
- Hiemstra, J. F., & Rijsdijk, K. F. (2003). Observing artificially induced strain: implications for subglacial deformation. *Journal of Quaternary Science*, 18, 373–383.
- Hiemstra, J. F., & van der Meer, J. J. M. (1997). Pore-water controlled grain fracturing as an indicator for sub glacial shearing in tills. *Journal of Glaciology*, 43, 446–454.
- Hooke, R. L., & Iverson, N. R. (1995). Grain-size distribution in deforming subglacial tills: Role of grain fracture. *Geology*, 23, 57–60.
- Hooke, R. L., & Jennings, C. E. (2006). On the formation of the tunnel valleys of the southern Laurentide ice sheet. *Quaternary Science Reviews*, 25, 1364–1372.
- Hug, J. (1907). Geologie der nördlichen Teile des Kantons Zürich und der angrenzenden Gebiete. *Beiträge zur geologischen Karte der Schweiz (N. F.), 15. Lieferung*. Geologische Kommission der Schweizerischen Naturforschenden Gesellschaft.
- Hug, J., & Beilick, A. (1934). Die Grundwasserverhältnisse des Kantons Zürich. *Beiträge zur Geologie der Schweiz. Geotechnische Serie—Hydrologie. 1. Lieferung*. Geotechnische Kommission der Schweizerischen Naturforschenden Gesellschaft.
- Huntley, D. J., & Baril, M. R. (1997). The K content of the K-feldspars being measured in optical dating or in thermoluminescence dating. *Ancient TL*, 15, 11–14.
- Isler, A., Pasquier, F., Huber, M., & Kleboth, P. (1984). Geologische Karte der zentralen Nordschweiz, 1:100'000 (mit angrenzenden Gebieten von Baden-Württemberg). *Nagra Technischer Bericht NTB 84-25*. Wettingen: Nagra.
- Ivy-Ochs, S., Kerschner, H., Reuther, A., Preusser, F., Heine, K., Maisch, M., et al. (2008). Chronology of the last glacial cycle in the European Alps. *Journal of Quaternary Science*, 23, 559–573.
- Ivy-Ochs, S., Schäfer, J., Kubik, P. W., Synal, H.-A., & Schlüchter, C. (2004). Timing of deglaciation on the northern Alpine foreland (Switzerland). *Eclogae Geologicae Helveticae*, 97, 47–55.
- Jordan, P. (2010). Analysis of overdeepened valleys using the digital elevation model of the bedrock surface of Northern Switzerland. *Swiss Journal of Geosciences*, 103, 375–384.
- Jung, P. G. (1969). Beiträge zur Morphogenese des Zürcher Oberlandes im Spät- und Postglazial. Mit besonderer Berücksichtigung des Greifen- und Pfäffikersees. *Vierteljahrsschrift der Naturforschenden Gesellschaft in Zürich*, 114, 293–406.
- Keller, O., & Krayss, E. (2005). Der Rhein-Linth-Gletscher im letzten Hochglazial. 1. Teil: Einleitung, Aufbau und Abschmelzen des Rhein-Linth-Gletschers im Oberen Würm. *Vierteljahrsschrift der Naturforschenden Gesellschaft in Zürich*, 150, 19–32.
- Keller, O., & Krayss, E. (2010). Mittel- und spätpleistozäne Stratigraphie und Morphogenese in Schlüsselregionen der Nordschweiz. *Quaternary Science Journal*, 59, 88–119.
- Kempf, T., Freimoser, M., Haldimann, P., Longo, V., Müller, E., Schindler, C., Styger, G., & Wyssling, L. (1986). Die Grundwasservorkommen im Kanton Zürich, Erläuterungen zur Grundwasserkarte 1:25'000. *Beiträge zur Geologie der Schweiz. Geotechnische Serie*, 69. Schweizerische Geotechnische Kommission.
- Knighton, D. (1998). *Fluvial forms and processes. A new perspective*. London: Hodder Education.
- Kühni, A., & Pfiffner, O. (2001). The relief of the Swiss Alps and adjacent areas and its relation to lithology and structure: topographic analysis from a 250-m DEM. *Geomorphology*, 41, 285–307.
- Letsch, D., Winkler, W., von Quadt, A., & Gallhofer, D. (2015). The volcano-sedimentary evolution of a post-Variscan intramontane basin in the Swiss Alps (Glarus Verrucano) as revealed by zircon U–Pb age dating and Hf isotope geochemistry. *International Journal of Earth Sciences*, 104, 123–145.
- Lisiecki, L. E., & Raymo, M. E. (2005). A Pliocene–Pleistocene stack of 57 globally distributed benthic $\delta^{18}O$ records. *Paleoceanography* 20, PA1003.
- Longo, V. (1978). Geologie des Hagenholztunnels bei Kloten. *Eclogae Geologicae Helveticae*, 71, 175–182.
- Lowick, S. E., Buechi, M. W., Gaar, D., Graf, H. R., & Preusser, F. (2015). Luminescence dating of Middle Pleistocene proglacial deposits from northern Switzerland: Methodological aspects and stratigraphical conclusions. *Boreas*, 44, 459–482.
- Lukas, S., Benn, D. I., Boston, C. M., Brook, M., Coray, S., Evans, D. J., et al. (2013). Clast shape analysis and clast transport paths in glacial environments: A critical review of methods and the role of lithology. *Earth-Science Reviews*, 121, 96–116.
- Maizels, J. (1993). Lithofacies variations sandur deposits: The role of runoff regime, flow dynamics, and sediment supply characteristics. *Sedimentary Geology*, 85, 299–325.
- Matousek, F., Wanner, M., Baumann, A., Graf, H. R., Nüesch, R., & Bitterli, T. (2000). *Geologischer Atlas der Schweiz. 1050 Zurzach (Atlasblatt 102)*. Wabern: Bundesamt für Landestopografie.
- Menzies, J. (1989). Subglacial hydraulic conditions and their possible impact upon subglacial bed formation. *Sedimentary Geology*, 62, 125–150.
- Menzies, J. (2000). Micromorphological analyses of microfibrils and microstructures indicative of deformation processes in glacial sediments. *Geological Society London, Special Publications*, 176, 245–257.
- Menzies, J., & Ellwanger, D. (2011). Insights into subglacial processes inferred from the micromorphological analyses of complex diamicton stratigraphy near Illmensee-Lichtenegg, Höchst, Germany. *Boreas*, 40, 271–288.
- Menzies, J., van der Meer, J., & Rose, J. (2006). Till—as a glacial “tectomict”, its internal architecture, and the development of a “typing” method for till differentiation. *Geomorphology*, 75, 172–200.
- Menzies, J., & Zaniewski, K. (2003). Microstructures within a modern debris flow deposit derived from Quaternary glacial diamicton—a comparative micromorphological study. *Sedimentary Geology*, 157, 31–48.
- Murray, A. S., Thomsen, K. J., Masuda, N., Buylaert, J. P., & Jain, M. (2012). Identifying well-bleached quartz using the different bleaching rates of quartz and feldspar luminescence signals. *Radiation Measurements*, 47, 688–695.
- Murray, A. S., & Wintle, A. G. (2000). Luminescence dating of quartz using an improved single-aliquot regenerative-dose protocol. *Radiation Measurements*, 32, 57–73.
- Murray, A. S., & Wintle, A. G. (2003). The single aliquot regenerative dose protocol: Potential for improvements in reliability. *Radiation Measurements*, 37, 377–381.
- Pavoni, N., Jäckli, H., & Schindler, C. (1992). *Geologischer Atlas der Schweiz. 1091 Zürich (Atlasblatt 90)*. Wabern: Bundesamt für Landestopografie.
- Pavoni, N., Schindler, C., Freimoser, M., Haldimann, P., & Letsch, D. (2015). *Geologischer Atlas der Schweiz. 1091 Zürich (Atlasblatt 90). Erläuterungen*. Wabern: Bundesamt für Landestopografie.

- Penck, A. (1905). Glacial features in the surface of the Alps. *The Journal of Geology*, 13, 1–19.
- Penck, A., & Brückner, E. (1909). *Die Alpen im Eiszeitalter*. Leipzig: C. H. Tauchnitz.
- Phillips, E. (2006). Micromorphology of a debris flow deposit: Evidence of basal shearing, hydrofracturing, liquefaction and rotational deformation during emplacement. *Quaternary Science Reviews*, 25, 720–738.
- Pietsch, J., & Jordan, P. (2014). Digitales Höhenmodell Basis Quartär der Nordschweiz—Version 2014 und ausgewählte Auswertungen. *Nagra Technischer Bericht NAB 14-02*. Wettingen: Nagra.
- Piotrowski, J. A. (1994). Tunnel-valley formation in northwest Germany—Geology, mechanisms of formation and subglacial bed conditions for the Bornhöved tunnel valley. *Sedimentary Geology*, 89, 107–141.
- Powers, M. C. (1953). A new roundness scale for sedimentary particles. *Journal of Sedimentary Petrology*, 23, 117–119.
- Prescott, J. R. & Hutton, J. T. (1994). Cosmic ray contributions to dose rates for luminescence and ESR dating: large depths and long-term time variations. *Radiation Measurements*, 23, 497–500.
- Preusser, F. (2004). Towards a chronology of the Late Pleistocene in the northern Alpine Foreland. *Boreas*, 33, 195–210.
- Preusser, F., & Degering, D. (2007). Luminescence dating of the Niederweningen mammoth site, Switzerland. *Quaternary International*, 164–165, 106–112.
- Preusser, F., Drescher-Schneider, R., Fiebig, M., & Schlüchter, C. (2005). Re-interpretation of the Meikirch pollen record, Swiss Alpine Foreland, and implications for Middle Pleistocene chronostratigraphy. *Journal of Quaternary Science*, 20, 607–620.
- Preusser, F., & Graf, H. (2002). Erste Ergebnisse von Lumineszenzdatierungen eiszeitlicher Ablagerungen der Nordschweiz. *Jahresberichte und Mitteilungen des Oberrheinischen Geologischen Vereins*, 84, 419–438.
- Preusser, F., Graf, H. R., Keller, O., Krayss, E., & Schlüchter, C. (2011). Quaternary glaciation history of northern Switzerland. *E & G Quaternary Science Journal*, 60, 282–305.
- Preusser, F., & Kasper, H. U. (2001). Comparison of dose rate determination using high-resolution gamma spectrometry and inductively coupled plasma-mass spectrometry. *Ancient TL*, 19, 17–21.
- Preusser, F., Reitner, J., & Schlüchter, C. (2010). Distribution, geometry, age and origin of overdeepened valleys and basins in the Alps and their foreland. *Swiss Journal of Geosciences*, 103, 407–426.
- Rades, E. F., Fiebig, M., & Lüthgens, C. (2016). Luminescence dating of the Rissian type section in southern Germany as a base for correlation. *Quaternary International*. <https://doi.org/10.1016/j.quaint.2016.07.055>. (in press).
- Rey, R., Wildberger, A., Frank, S., & Freimoser, M. (2011). *Geologischer Atlas der Schweiz. 1072 Winterthur (Atlasblatt 140)*. Wabern: Bundesamt für Landestopografie.
- Rose, J., & Menzies, J. (2002). Glacial stratigraphy. In J. Menzies (Ed.), *Modern and past glacial environments* (pp. 445–473). Oxford: Butterworth-Heinemann.
- Salcher, B. C., Kober, F., Kissling, E., & Willett, S. D. (2014). Glacial impact on short-wavelength topography and long-lasting effects on the denudation of a deglaciated mountain range. *Global and Planetary Change*, 115, 59–70.
- Salcher, B. C., Starnberger, R., & Götz, J. (2015). The last and penultimate glaciation in the North Alpine Foreland: New stratigraphical and chronological data from the Salzach glacier. *Quaternary International*, 388, 218–231.
- Schlüchter, C. (1977). Grundmoräne versus Schlammmoräne—Two types of lodgement till in the Alpine Foreland of Switzerland. *Boreas*, 6, 181–188.
- Schlüchter, C. (1979). Übertiefe Talabschnitte im Berner Mittelland zwischen Alpen und Jura (Schweiz). *Eiszeitalter und Gegenwart*, 29, 101–113.
- Schlüchter, C. (1989). The most complete Quaternary record of the Swiss alpine foreland. *Palaeogeography, Palaeoclimatology, Palaeoecology*, 72, 141–146.
- Schlüchter, C. (1997). Sedimente des Gletschers (Teil I). *Bulletin für angewandte Geologie*, 2, 99–112.
- Schlunegger, F., & Norton, K. P. (2013). Water versus Ice: The competing roles of modern climate and Pleistocene glacial erosion in the Central Alps of Switzerland. *Tectonophysics*, 602, 370–381.
- Siegenthaler, C., & Huggenberger, P. (1993). Pleistocene Rhine gravel: deposits of a braided river system with dominant pool preservation. *Geological Society, London, Special Publications*, 75, 147–162.
- Sneed, E. D., & Folk, R. L. (1958). Pebbles in the Lower Colorado River, Texas. A study in particle morphogenesis. *The Journal of Geology*, 66, 114–150.
- Sommerhalder, E. R. (1968). *Glazialmorphologische Detailuntersuchungen im hochwürdig-eiszeitlich vergletscherten unteren Glattal (Kanton Zürich)*. Ph.D. dissertation, Universität Zürich.
- Starnberger, R., Drescher-Schneider, R., Reitner, J. M., Rodnigh, H., Reimer, P. J., & Spötl, C. (2013). Late Pleistocene climate change and landscape dynamics in the Eastern Alps: The inner-alpine Unterangerberg record (Austria). *Quaternary Science Reviews*, 68, 17–42.
- Stein, M. (1948). *Morphologie des Glattales*. Ph.D. dissertation, Universität Zürich.
- Suter, H. (1944). Glazialgeologische Studien im Gebiet zwischen Limmat, Glatt und Rhein. *Eclogae Geologicae Helveticae*, 37, 83–97.
- Trümpy, R. & Dössegger, R. (1973). Permian of Switzerland. In: Falke, H. (Ed), *Rotliegend, Essays on European Lower Permian* (pp. 189–215). International Sedimentary Petrography Series 15. Leiden: Brill.
- van der Meer, J. J. M., & Menzies, J. (2011). The micromorphology of unconsolidated sediments. *Sedimentary Geology*, 238, 213–232.
- van Husen, D. (1979). Verbreitung, Ursachen und Füllung glazial übertiefer Talabschnitte an Beispielen in den Ostalpen. *Eiszeitalter und Gegenwart*, 29, 9–22.
- Weber, J. (1901). Beiträge zur Geologie der Umgebung des Pfäffikersees. *Mitteilungen der Naturforschenden Gesellschaft Winterthur*, 3, 142–176.
- Weber, A. (1928). Die Glazialgeologie des Tösstales und ihre Beziehung zur Diluvialgeschichte der Nordostschweiz. *Mitteilungen der Naturwissenschaftlichen Gesellschaft Winterthur*, 17, 1–92.
- Weber, A. (1934). Zur Glazialgeologie des Glattales. *Eclogae Geologicae Helveticae*, 27, 3–43.
- Welten, M. (1982). Pollenanalytische Untersuchungen im Jüngeren Quartär des nördlichen Alpenvorlandes der Schweiz. *Beiträge zur Geologischen Karte der Schweiz*, 156. Schweizerische Geologische Kommission.
- Wyssling, G. (2008). *Geologischer Atlas der Schweiz. 1092 Uster (Atlasblatt 128). Erläuterungen*. Wabern: Bundesamt für Landestopografie.
- Wyssling, L., & Wyssling, G. (1978). Interglaziale See-Ablagerungen in einer Bohrung bei Uster (Kanton Zürich). *Eclogae Geologicae Helveticae*, 71, 357–375.
- Yanites, B. J., Ehlers, T. A., Becker, J. K., Schnellmann, M., & Heuberger, S. (2013). High magnitude and rapid incision from river capture: Rhine river, Switzerland. *Journal of Geophysical Research: Earth Surface*, 118, 1060–1084.
- Zhang, Z., Pfrang, G. & Amstutz, G. (1981). New observations on the formation of spilites and keratophyres of Glarus, Switzerland

- (with special reference to material in the moraines of the Linth glacier). *Schweizerische mineralogische und petrographische Mitteilungen*, 61, 219–235.
- Zingg, T. (1934). *Geologischer Atlas der Schweiz. Mönchaldorf–Hinwil–Wädenswil–Rapperswil (Atlasblatt 7). Erläuterungen*. Geologische Kommission der Schweizerischen Naturforschenden Gesellschaft.
- Zingg, T. (1935). Beitrag zur Schotteranalyse: die Schotteranalyse und ihre Anwendung auf die Glattalschotter. *Schweizerische Mineralogische und Petrographische Mitteilungen*, 15, 39–140.